



Universitetet  
i Stavanger

**PETTER TESDAL**

SUPERVISORS: DIMITRIOS PAVLOU, ATLE SJØLYST-KVERNELAND

---

# Static Structural FE Analysis on Two S355MC Frames

In Cooperation with TKS AGRI AS

---

**Bachelor Thesis 2024**

**Mechanical Engineering**

**Institutt for maskin, bygg og materialteknologi**

**Det teknisk-naturvitenskapelige fakultet**



Private photo taken at  
TKS AGRI AS

# Abstract

This thesis deals with finite element static structural analyses on two S355MC steel frames. The first frame is developed by TKS AGRI AS and is currently in use in various agricultural feed- processor and distribution machines. The company is considering reducing the size of the frame and consequently the material consumption. The second frame is a digital design proposal to achieve these goals. The finite element simulations create a basis for determining if the original frame is oversized and whether the optimized frame can carry the same load as the original.

Both frames are analyzed similarly using Ansys Mechanical within the Ansys Workbench environment. The frames should withstand a vertical feed load of 2000 kg and a machine mass of 700 kg while being supported by four floor stands. The analysis outputs are displacements and Von Mises Stress.

The results indicate a generally high safety factor above 2.6 against yielding for the main side plates on the original frame, showing that a size reduction of these is relevant. The reduced side plates on the optimized frame also show general low stresses. Therefore, the size reduction was successful. However, stress concentrations at contact points, welds, and bolt connections exceed the yield limit. Relevant improvement proposals are given, like using rounded edges, mounting extra reinforcement plates, and using larger bolts. The results also displays relatively large displacements of 9,8 mm on the optimized frame where the feed load is applied. To counteract this, it is proposed to use modified cross-sections for the profiles carrying the load and mounting extra members participating in carrying the load.

# Table of Contents

## **1. Introduction**

## **2. Theory**

- 2.1 Finite Element Method
- 2.2 Advantages and disadvantages of FEM
- 2.3 Principles of FEM
- 2.4 Von Mises Stress
- 2.5 Contact stresses in bolt holes

## **3. Project definitions**

- 3.1 Geometry overview
- 3.2 Limitations
- 3.3 Materials
- 3.4 Boundary conditions
- 3.5 Loads
- 3.6 Other assumptions

## **4. Methodology**

## **5. Results**

- 5.1 Displacements: original frame
- 5.2 Von Mises stress: original frame
- 5.3 Displacements: optimized frame
- 5.4 Von Mises stress: optimized frame

## **6. Discussion**

- 6.1 Validity of results
- 6.2 Reasonability of results
- 6.3 Results in relevant regions assessed
  - 6.3.1 Side plates on the original frame
  - 6.3.2 Side plates on the optimized frame
  - 6.3.3 Area of maximum displacements
  - 6.3.4 Bolt holes in side plates
  - 6.3.5 Other contact points
  - 6.3.6 Weldments

## **7. Conclusion**

## **8. References**

## **Acknowledgements**

## **Appendix**

- A.1 Geometry overview original frame
- A.2 Geometry overview optimized frame
- A.3 Bolt/hole contact stress calculation 1
- A.4 Bolt/hole contact stress calculation 2 using triple plate thickness and doubled size bolts/holes
- A.5 Comparison FEM results with analytic calculations: Normal stress at the middle length of a simple beam
- A.6 Comparison FEM results with analytic calculations: Normal stress at the  $\frac{1}{4}$  length of a simple beam
- A.7 Equilibrium check for original frame

# 1. Introduction

The project is carried out through the mechanical engineering study program at the University of Stavanger and in cooperation with TKS AGRI AS in the spring of 2024. In advance, I was on internship at TKS AGRI as part of a practical course in the autumn of 2023. With goodwill from the firm's manager, I was granted the opportunity to write my thesis on a self-chosen subject within the firm's area of operation. Alongside the internship period, I was enrolled in a course on the finite element method at UiS. I decided to center my project around a finite element analysis on a steel frame that I became familiar with through the internship. I contacted both the lecturer of the FEM course and the firm's manager, and both agreed to be supervisors.

The frame dealt with in this project is part of various feed-handling machines that are in use on many farms today, like K2 CombiCutter and Magazine R2. The K2 CombiCutter is a grass bale cutter used to prepare feed for cattle and other livestock. The dense bales are processed through a drum with knives and the machine outputs loose feed that is ready to be distributed for the animals to eat. The distribution among the animals is carried out by other machines, typically a belt system. The K2 CombiCutter will generally not be loaded with more than one bale at a time.



Figure 1.1 K2 CombiCutter. Side plate of frame highlighted with stapled white lines. Private photo.



Figure 1.2 Inside K2 CombiCutter. Grey cutting drum with knives. The floor is the top of the frame. Chain-driven transport function which moves the feed towards the drum. Private photo.

To plan the feeding process and work efficiently, the farmer is interested in stocking up on bales that are ready to be cut when needed. R2 Magazine serves this storage function. The magazine can be positioned such that the platform on the K2 CombiCutter is extended. In this way, feed can be stored for some days, and one does not have to load new bales for each feeding session. Chain-driven transport functions on both machines move the bales towards the drum on the K2 CombiCutter whenever feeding shall occur. R2 Magazine can support the load of two bales at a time.



*Figure 1.3 R2 Magazine with a long version of the frame. Otherwise similar to the frame on K2 CombiCutter. Private photo.*



*Figure 1.4 Frames in the production line. Private photo.*

The company wants to know if the frame used in these machines is oversized and is interested in finding out if a smaller frame could perform equally well under the same load. This would reduce material consumption, which is directly related to cost, and the machine would also take less space. Emphasis is put upon the size of the main side plates and TKS AGRI has provided dimensions for the shrinking of these, fig.1.5. The overall purpose of this thesis is therefore to propose an optimized smaller frame design adjusted to these dimensions and test for stresses and displacements, both for the original and for the new frame. The results give two indications: 1) if the original frame is oversized, and 2) if the optimized frame can handle the same loading situation as the original.

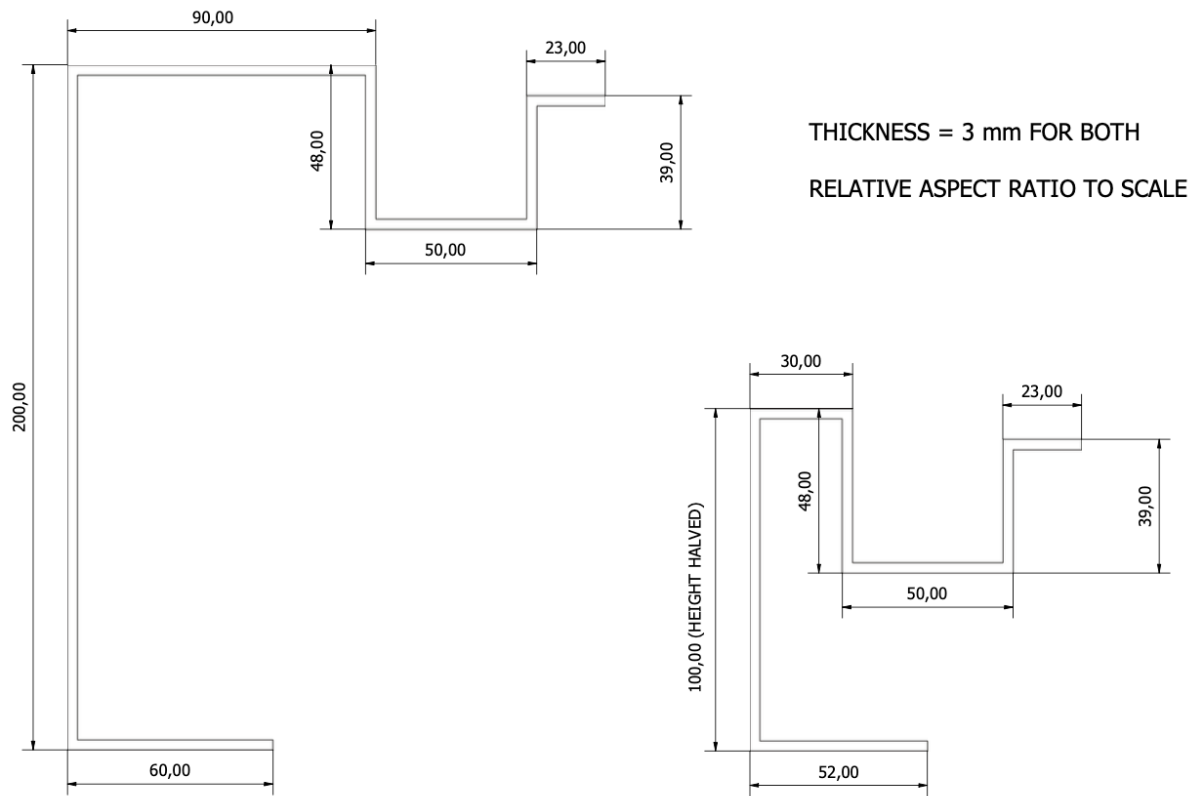


Figure 1.5 Left: original cross section for the main side plates on the frame. Right: New dimensions based on TKS AGRI's provided dimensions used in the optimized frame. Drawing produced in Autodesk Inventor Professional [15].



## **2. Theory**

### **2.1 Finite element method**

The finite element method (FEM) is a numerical method used in technical calculations on constructions, flow of liquids, heat flow and more [1, p.xiii], [1, p.1]. A brief overview of the finite element method for calculating displacements in structural constructions is given in paragraphs below. These types of calculations are relevant for civil engineers, mechanical engineers and others who need to determine an approximate picture of the behavior of their structural or mechanical design after external load is applied. A stress analysis is particularly helpful as stress information can be connected to material information to determine whether any plastic deformation will occur. For the analyst, time is usually spent on formulating the problem and interpreting the results, while computers solve large systems of linear equations.

### **2.2 Advantages and disadvantages of FEM**

FEM computer programs are efficient tools for validating mechanical and structural designs. In the process of concept generation, each concept can be tested individually, and the results compared. As all designing and testing is digital, one can avoid costs and time in making physical prototypes for testing. However, since the method is approximate [1, p.1], it does not fully replace other forms of design validation.

As just mentioned, the FE method is approximate. The structure under consideration and its loads are modeled in a simplified manner. An evenly distributed load may for example be used as a simplification of a complex load situation and inappropriate number of elements meshing the shapes can lead to misleading results [1, p.1]. The FE method can therefore be seen as an approximate simulation tool.

## 2.3 Principles of FEM

A structural FEM problem is generally characterized by four knowns that are used to relieve two unknowns. The four knowns are structure geometry, material data, external forces and supports. The aim is to calculate stresses and displacements at every location within the structure. These are the two unknowns - the stresses and the displacements. [3] In this subchapter, finding the displacement field of a structure is considered.

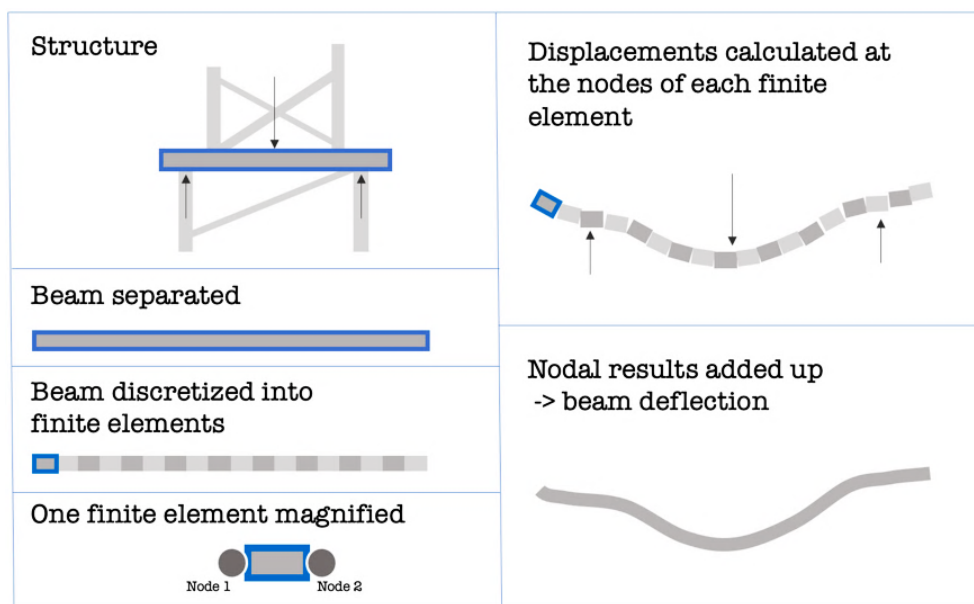


Figure 2.3.1 Illustration: FEM procedure finding deflection of a beam. Inspired by clip 4:07 from [17].

Instead of using analytical formulas to calculate displacements in the members making up a structure, the FE method involves discretizing the members into finite elements that mesh the shapes, as shown in fig. 2.3.1. Each FE has two or more endpoints, called nodes. The external forces acting on the structure are distributed between the small elements as internal forces on the nodes. The displacements of each FE's nodes are found by use of stiffness equations that correlate the nodal internal forces to the nodal displacements [1, p.2]. The summation of the displacements of all the finite elements provides the overall deformation of the structure under consideration. This is done by polynomial interpolation between the nodes of the finite elements [1, p.1].




The general formulation of a stiffness equation is

$$[1, \text{p.6}] \quad \{r\} = [k]\{d\} \quad (2.3.1)$$

where  $\{r\}$  is a list of internal forces acting on the nodes of the element,  $[k]$  is a stiffness matrix that describe the element's resistance to deformation and  $\{d\}$  is a list of nodal displacements [1, p.6]. It is material- and geometry properties included in the stiffness matrix  $[k]$  that determine how resistant the element is to deformation [1, p. 2].

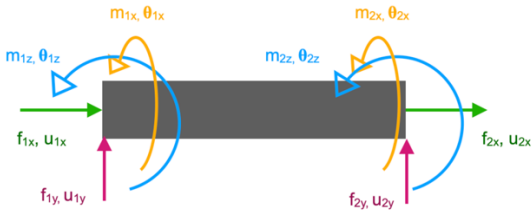
Table 2.3.1 provides some examples of stiffness equations for a 2d-beam element with nodes named 1 and 2 subjected to different loads. Axial forces cause axial elongation or contraction, shear forces cause displacement normal to the beam axis, bending moments lead to bending and torsional moments cause twisting. The stiffness equations in table 2.3.1 are based on mechanics theory on the material behavior due to these types of loads and the principle of equilibrium [1, p. 41], [1, p. 61].  $E$ ,  $A$ ,  $L$ ,  $I_z$ ,  $G$  and  $J$  represent Young's modulus [1, p.57], cross sectional area [1, p.57], element length [1, p.57], moment of inertia [1, p.200], shear modulus [1, p.192] and polar moment of inertia [1, p.192], respectively. The  $f$ 's,  $m$ 's,  $u$ 's and  $\theta$ 's, are nodal forces [1, p.61], bending- and torsional moments [1, p.154], [1, p.193], linear displacements [1, p.154], and rotational displacements [1, p.154], respectively.

Table 2.3.1 Stiffness equations for each type of load a 2d-beam element can be subjected to. Loads and displacement variables are indicated in the diagrams.

Diagram	Stiffness equation
 <p>Axial forces</p> <p>Figure retrieved from [2, p.6], based on figure 6.12 in [1, p.195]</p>	$\begin{Bmatrix} f_{1x} \\ f_{2x} \end{Bmatrix} = \begin{bmatrix} \frac{EA}{L} & -\left(\frac{EA}{L}\right) \\ -\left(\frac{EA}{L}\right) & \frac{EA}{L} \end{bmatrix} \begin{Bmatrix} u_{1x} \\ u_{2x} \end{Bmatrix}$ <p>[1, p.194]</p>
 <p>Bending moments and shear forces</p> <p>Figure retrieved from [2, p.6], based on figure 6.12 in [1, p.195]</p>	$\begin{Bmatrix} f_{1y} \\ m_{1z} \\ f_{2y} \\ m_{2z} \end{Bmatrix} = \frac{EI_z}{L^3} \begin{bmatrix} 12 & 6L & -12 & 6L \\ 6L & 4L^2 & -6L & 2L^2 \\ -12 & -6L & 12 & -6L \\ 6L & 2L^2 & -6L & 4L^2 \end{bmatrix} \begin{Bmatrix} u_{1y} \\ \theta_{1z} \\ u_{2y} \\ \theta_{2z} \end{Bmatrix}$ <p>[1, p.194]</p>
 <p>Torsional moments</p> <p>Figure retrieved from [2, p.6], based on figure 6.12 in [1, p.195]</p>	$\begin{Bmatrix} m_{1x} \\ m_{2x} \end{Bmatrix} = \begin{bmatrix} \frac{GJ}{L} & -\left(\frac{GJ}{L}\right) \\ -\left(\frac{GJ}{L}\right) & \frac{GJ}{L} \end{bmatrix} \begin{Bmatrix} \theta_{1x} \\ \theta_{2x} \end{Bmatrix}$ <p>[1, p.195]</p>

For a FE subjected to various types of loads, the different stiffness equations corresponding to each type of load can be combined into a new matrix equation called the element equation [1, p.195]. For a 2d-beam element subjected to all the types of loads presented in table 2.3.1 (axial forces, shear forces, bending moments and torsional moments), the stiffness equations can be combined into the element equation shown in table 2.3.2.

Table 2.3.2 Element equation for a 2d-beam element

Diagram	Element equation
 <p>Axial forces, shear forces, bending moments and torsional moments</p> <p>Figure retrieved from [2, p.7], based on figure 6.12 in [1, p.195]</p>	$\begin{Bmatrix} f_{1x} \\ f_{1y} \\ m_{1z} \\ m_{1x} \\ f_{2x} \\ f_{2y} \\ m_{2z} \\ m_{2x} \end{Bmatrix} = \begin{bmatrix} \frac{EA}{L} & 0 & 0 & 0 & -\left(\frac{EA}{L}\right) & 0 & 0 & 0 \\ 0 & \frac{12EI_z}{L^3} & 0 & \frac{6EI_z}{L^2} & 0 & -\left(\frac{12EI_z}{L^3}\right) & 0 & \frac{6EI_z}{L^2} \\ 0 & 0 & \frac{GJ}{L} & 0 & 0 & 0 & -\left(\frac{GJ}{L}\right) & 0 \\ 0 & \frac{6EI_z}{L^2} & 0 & \frac{4EI_z}{L} & 0 & -\left(\frac{6EI_z}{L^2}\right) & 0 & \frac{2EI_z}{L} \\ -\left(\frac{EA}{L}\right) & 0 & 0 & 0 & \frac{EA}{L} & 0 & 0 & 0 \\ 0 & -\left(\frac{12EI_z}{L^3}\right) & 0 & -\left(\frac{6EI_z}{L^2}\right) & 0 & \frac{12EI_z}{L^3} & 0 & -\left(\frac{6EI_z}{L^2}\right) \\ 0 & 0 & -\left(\frac{GJ}{L}\right) & 0 & 0 & 0 & \frac{GJ}{L} & 0 \\ 0 & \frac{6EI_z}{L^2} & 0 & \frac{2EI_z}{L} & 0 & -\left(\frac{6EI_z}{L^2}\right) & 0 & \frac{4EI_z}{L} \end{bmatrix} \begin{Bmatrix} u_{1x} \\ u_{1y} \\ \theta_{1z} \\ \theta_{1x} \\ u_{2x} \\ u_{2y} \\ \theta_{2z} \\ \theta_{2x} \end{Bmatrix}$ <p>[1, p.195]</p>

The element equation applies to one element. However, the analyst wants to solve for displacement values throughout structures that consist of many elements, like a beam discretized to hundreds of finite elements or a frame consisting of various discretized members [2, p.7]. To arrive at a system of linear equations that describe the whole structure, the element equations for every node in the structure should be added together. That is only possible when the element equations share the same variables [2, p.7], [3]. To achieve this, all element equations are further expanded to the degrees of freedom of the whole structure [1, p. 223]. This involves including all possible loads and displacements acting on every node of the structure in each element equation [2, p.7]. Loads and displacements that are not relevant to the element under consideration, is accounted for by zero-entries in the stiffness matrices [2, p.7]. The summation of the expanded element equations results in a global stiffness equation,

$$[1, p.44] \quad \{R\} = [K]\{d\}. \quad (2.3.2)$$

The (capital)  $\{R\}$  represents a list of resultant forces at each node [1, p.44], the (capital)  $[K]$  is a stiffness matrix for the whole structure and  $\{d\}$  is the displacement field of the structure. The system is not solvable unless boundary conditions for displacements and external forces are applied.

An example on boundary conditions is illustrated in figure 2.3.2. The diagram depicts a cantilevered and discretized beam. Since the beam is fix-supported to the wall at the left end, the first node will not move, bend, or twist in any direction. Therefore, regarding the beam as 2D, four BCs for displacement applies here;  $u_{1x} = 0$ ,  $u_{1y} = 0$ ,  $\theta_{1x} = 0$  and  $\theta_{1z} = 0$ . At the right end, the displacement is not known. That is yet to be calculated. However, a boundary condition for external force is known. At the 100<sup>th</sup> node, a concentrated vertical force of 10 kN is acting. Therefore, one BC for external forces applies here;

$$F_{100y} = -10 \text{ kN}.$$

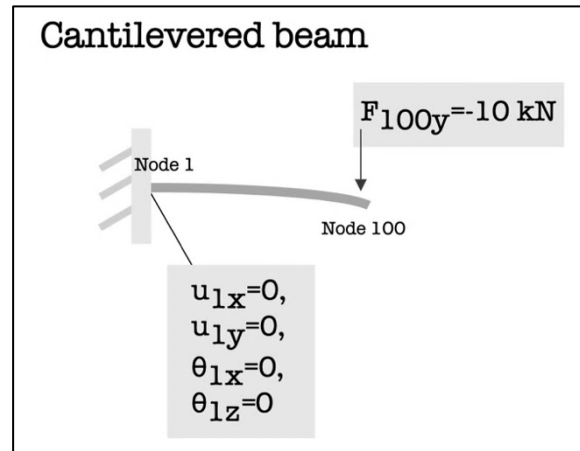


Figure 2.3.2 Illustration: Cantilevered beam with known boundary conditions

Boundary conditions are formulated in two separate matrix equations. They have the following format:

$$\begin{aligned} [1, \text{p.48-49}] \quad [BCd]\{d\} &= \{DO\} \\ [BCR]\{R\} &= \{RO\} \end{aligned} \quad (2.3.3)$$

The matrices  $[BCd]$  (boundary conditions displacements) and  $[BCR]$  (boundary conditions external forces) specify which node and which degree of freedom to apply boundary conditions, while  $\{DO\}$  and  $\{RO\}$  contain the values of the BCs [2, p.8].

Lastly, the global element equation is combined with the boundary conditions to arrive at a solvable system for the displacement field of the structure [1, p.49]. By way of algebraic matrix operations, the format can be as follows:

$$[1, p.49] \quad \begin{bmatrix} [K] & [-I] \\ [BCd] & [BCR] \end{bmatrix} \begin{Bmatrix} \{d\} \\ \{R\} \end{Bmatrix} = \begin{Bmatrix} \{0\} \\ \{DO\} + \{RO\} \end{Bmatrix}. \quad (2.3.4)$$

$[-I]$  is a negative identity matrix and  $\{0\}$  is a zero matrix. Both have the same dimensions as the global stiffness matrix  $[K]$ . If every boundary condition is applied, the system should now be solvable. The computer solves the large linear algebraic system, and the result is the displacements of every node in the structure.

The displacement values are interesting as one can determine whether the deformation of the structure is acceptable or not. The displacement values can also be used to calculate internal forces and moments which further can be calculated in terms of stress [2, p.9], [1, p.7].

## 2.4 Von Mises stress

Von Mises stress is a common result output of a FE analysis. This stress type can be calculated at every node of the structure and can be displayed as Von Mises stress maps on the structure using computer programs.

Von Mises stress can be calculated using the general state of stress (fig. 2.4.1) that explains stresses acting within a body. It combines the nine stress varieties into one scalar that is comparable with the yield stress of the material. The advantage is that the Von Mises theory provides a simple yield criterion, even for a part under complex load. [5]

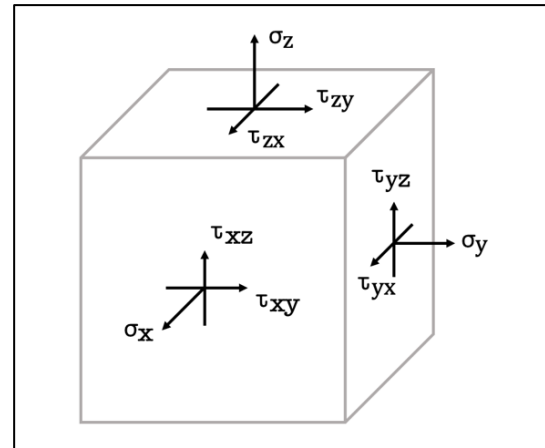


Figure 2.4.1 Illustration: general-state-of-stress cube.  
Figure based on Fig.1-11 in [4, p.41].

Yielding will likely occur if the Von Mises value is greater than the yield stress [7, p.250]. One formulation of Von Mises stress is given in eq. (2.4.1).

[7, p.251]

(2.4.1)

$$\sigma_v = \frac{1}{\sqrt{2}} \left[ (\sigma_x - \sigma_y)^2 + (\sigma_y - \sigma_z)^2 + (\sigma_z - \sigma_x)^2 + 6(\tau_{xy}^2 + \tau_{yz}^2 + \tau_{zx}^2) \right]^{\frac{1}{2}}$$



## 2.5 Contact stresses in bolt holes

Bolt connections represent sources of high stress concentrations because the forces here can be quite large, and they act on small areas. This subchapter explains an analytical method to calculate contact stresses between a bolt and the inner face of the hole in which it is mounted.

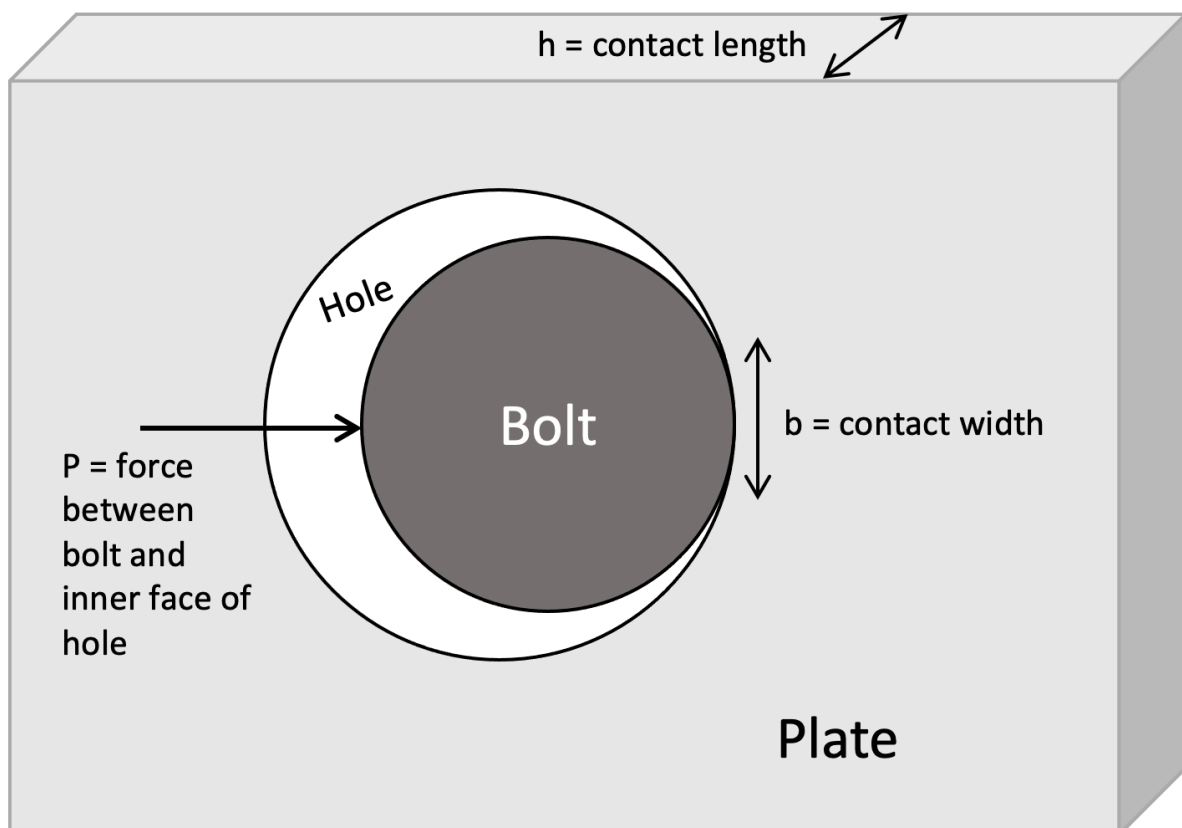


Figure 2.5.1 Illustration: Scenario for calculating contact stresses between a bolt and a hole in a plate. Based on figure 17.12 c) in [6, p. 611] and explanations from supervisor Dimitrios Pavlou

As shown in figure 2.5.1, a contact force  $P$  acts between the bolt shank and the inner face of the hole. Several equations are needed to calculate the contact stress and they are presented below.

The  $w$  in eq. (2.5.1) is the contact force per unit length [6, p.612], where  $h$  is the thickness of the plate.

$$[6, p. 612] \quad w = \frac{P}{h} \quad (2.5.1)$$

In eq. (2.5.2),  $R$  represents the radii of the hole/bolt. The bolt and hole deforms slightly when they are forced into contact which cause them to be in contact over an area opposed to a line, had they not been deformable [6, p. 592]. This deformation is taken into account by including the material properties  $\nu$  (Poisson's ratio) and  $E$  (Young's modulus) for both the plate and bolt in the equation.

$$[6, p. 612] \quad \Delta = \frac{1}{\left(\frac{1}{2R_{hole}}\right) + \left(\frac{1}{2R_{bolt}}\right)} \left( \frac{1 - \nu_{plate}^2}{E_{plate}} + \frac{1 - \nu_{bolt}^2}{E_{bolt}} \right) \quad (2.5.2)$$

$\Delta$  is used together with  $w$  to calculate the contact width  $b$  according to eq. (2.5.3).

$$[6, p. 612] \quad b = \sqrt{\frac{2w\Delta}{\pi}} \quad (2.5.3)$$

The maximum shear stress at the contact can be calculated according to eq. (2.5.4).

$$[6, p. 613] \quad \tau_{max} = 0.300 \left( \frac{b}{\Delta} \right) \quad (2.5.4)$$

There is danger of yielding if the maximum shear stress exceeds the half of the yield stress [7, p. 248]. For this yield criteria, eq. (2.5.5) computes the safety factor against yielding at the contact area between the hole and the bolt.

$$[7, p. 248] \quad SF = \frac{\sigma_{yield}/2}{\tau_{max}} \quad (2.5.5)$$

### 3. Project definitions

This part provides information on the geometry, limitations, materials, boundary conditions and loads that go into the FEM-simulations on the frames. Assumptions involved are also mentioned.

#### 3.1 Geometry overview

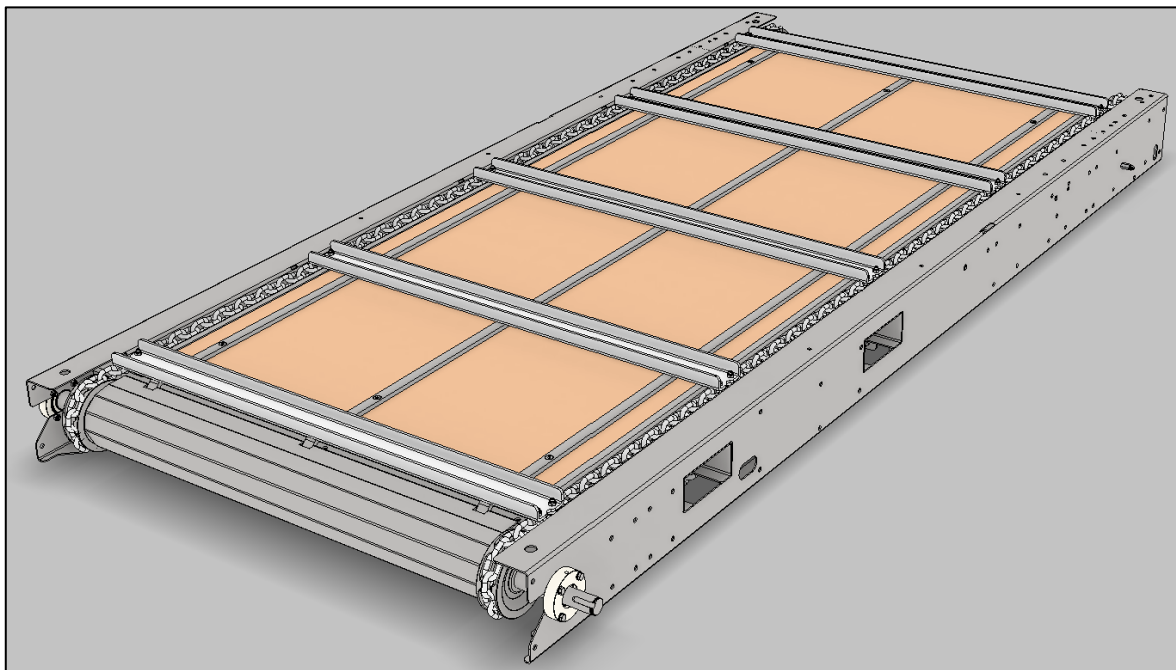


Figure 3.1.1 Original frame CAD assembly received from TKS AGRI AS. Screenshot from [15].

The original frame is approximately a three by 1,4 meter construction. It consists of various beam profiles, rails, a plywood plate etc. The main longitudinal side plates have a 3 mm thick profile that is laser-cut and bent. Between the side plates and under the plywood plate, there are five transverse beams: two hollow profiles, a custom profile and two C-profiles. All connected parts are fastened with welds or bolts. Exploded views of the parts used in the simplified version for the simulation as well as the modeled optimized frame can be found in the appendix.

## 3.2 Limitations

The simulations performed are static. That means that dynamic forces due to the frame's transport function and operation of the cutting drum is not considered. Moreover, fatigue calculations and corrosion wear are excluded. The scope is to determine deformations and Von Mises stress in the frames when static loads are applied. However, the feed load is increased to take into account the impact forces when the machine is loaded. This is mentioned in more detail in subchapter 3.5.

## 3.3 Materials

The metal parts of the frame is machined from S355MC steel. All weld material are assumed to be S355MC as well. The plywood plate is assigned material properties of plywood. Some important mechanical properties for these two materials are given in the table below. These values are used in the simulations.

Table 3.3.1 Material properties of S355MC and plywood. Sources: [16] and material library from [12], [13].

	<b>Use</b>	<b>Density</b>	<b>Elastic modulus</b>	<b>Poisson's ratio</b>	<b>Ultimate tensile strength</b>	<b>Yield stress</b>
<b>S355MC Structural Steel</b>	All beam profiles, rails, and welds	7,85 g/cm <sup>3</sup>	207,5 GPa	0,29	490 MPa	355 MPa
<b>Plywood</b>	Floor plate	0,748 g/cm <sup>3</sup>	6,320 MPa	0,245	56,1 MPa	38,1 MPa

### 3.4 Boundary conditions

The frame is supported different ways on different TKS AGRI machines, but this project is focused on stationary machines where the frame is supported by four floor stands. To simulate the feet, fixed supports are applied to bolt holes where the feet are mounted. These bolt holes are placed on the outer side of the frame.



Figure 3.4.1 Diagram showing bolt holes in the outer side of the frame where fixed supports are applied to simulate floor stands

### 3.5 Loads

The worst-case load for the frame is when two grass bales are placed on top of it. This loading situation is therefore simulated. The bales are assumed to be weighing 1000 kilograms each. On the farms, bales are usually lifted in place by a tractor-operated front loader. To account for the impact when the bales hit the frame, they are assumed to be dropped from a height of five centimeters in 0,5 seconds. This adds to the bale weight force and the resulting vertical force is 12000 N per bale.

The vertical forces due to the bales act over a delimited area and on various parts of the frame. The bale size is assumed to be 1075 mm both in the width and the diameter, which is the same dimension as the width of the plywood plate on the original frame. Since bales are quite deformable, it is assumed that 40% of the diameter is in contact with the frame. This gives a force area of 1075x430 square millimeters per bale. In the simulations, the force areas due to the bales are placed symmetrically and 870 mm apart.

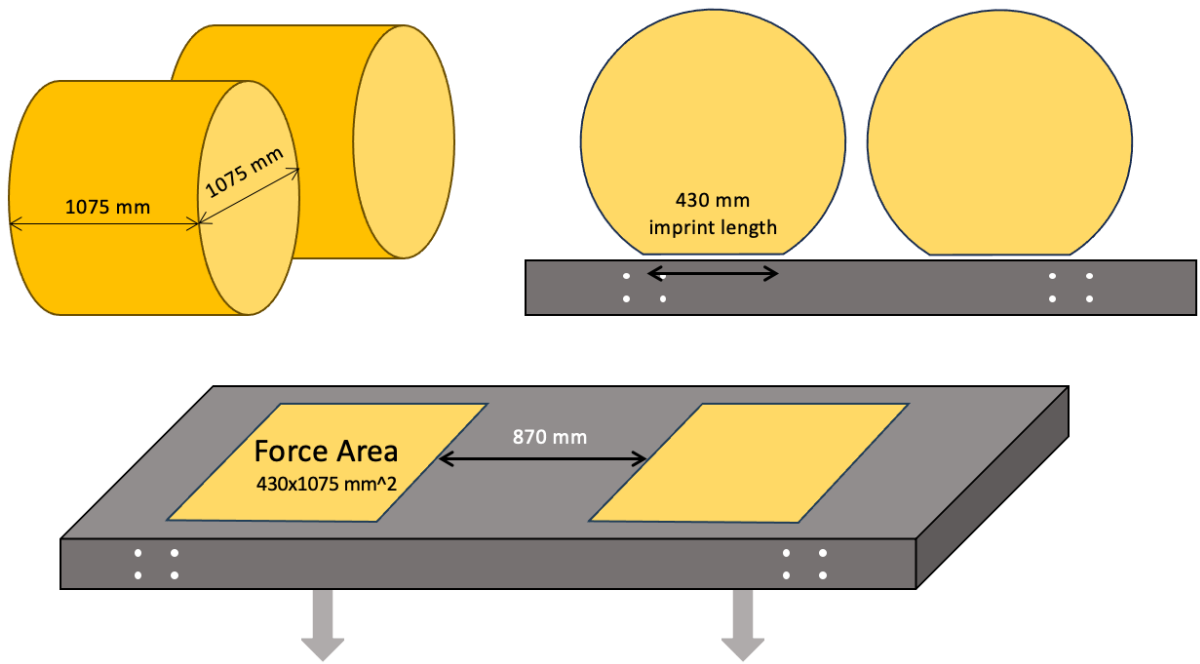


Figure 3.5.1 Diagrams explaining the areas where the bales' weight forces are applied

In addition to the feed load, the frame experiences weight forces from machine parts mounted on top of it. These parts include large side plates, cutting drum and more. The weight from these parts are assumed to sum 700 kg. The forces are applied on the outer sides of the frame, distributed evenly among five areas per side. Each force area represents 70 kg of load.

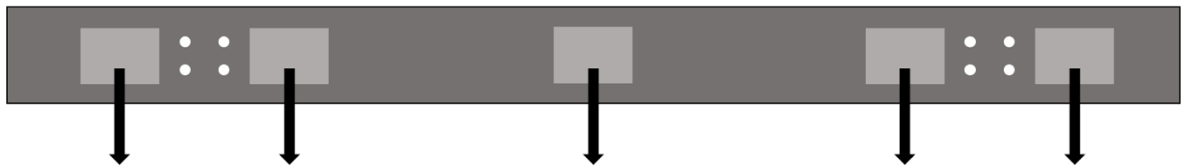


Figure 3.5.2 Diagram showing the machine weight distributed among five areas on the outer side of the frame

### 3.6 Other assumptions

The assumed friction coefficients for part contacts are 0,78 for steel on steel [8] and 0,4 for steel on wood [9], [10]. Welded parts are assumed to be completely bonded at the welds. That means that the parts are not allowed to separate or slide across each other at the welds [11]. Bolts fastening glide rails and the plywood plate to the frame are also simulated with such bonded contacts. These bolts and welds are therefore simulated “unbreakable”. The bolts fastening the frame to the floor stands are assumed to have a shank diameter of 10,5 mm. The gravitational acceleration is simplified to be  $10 \text{ m/s}^2$  in force calculations.

## 4. Methodology

The original frame's CAD model was received by TKS AGRI. In preparing the CAD model, the geometry was simplified. This included removing parts not necessary for the simulation and removing holes and fillets to make the parts simpler to mesh. In addition to the simplifications, there were some new features that were added. Welds were added according to weld drawings provided by the company and physical inspection on a real frame in the production line. Extra faces were drawn onto the frame where forces were to be applied. These CAD preparations were performed in Autodesk Inventor Professional [15] and Ansys SpaceClaim [14]. The optimized frame was modeled and welded in Autodesk Inventor Professional and prepared in Ansys SpaceClaim.

The CAD geometry was imported into a static structural workflow inside Ansys Workbench [12]. Within Ansys Mechanical, which is connected to the Ansys Workbench environment, the FEM analyses were set up. The steel and plywood materials were assigned to the right parts and necessary edits were done such that the properties of the steel material corresponded to S355MC. Automatically generated contacts were corrected for, ensuring that parts were only bonded at welds and bolt connections. Elsewhere, frictional contacts were applied. The mesh was generated based on "sizings" which in general specify how large the elements meshing the parts should be. Default brick elements of types SOLID186 and SOLID187 were used. Fixed supports were applied to the inner face of the bolt holes in the side plates of the frame. Forces were applied using the extra faces drawn onto the frames. After the simulations were solved, relevant screenshots were taken with results probed at different locations in the structures.



## 5. Results

The results are presented as screenshots from Ansys Mechanical [13].

The displacement results are shown in the form of color maps and previewed deformation on the structure. The units are in millimeters. The previewed deformation on the structure is exaggerated with a scale factor of 12. This means that a 3 mm displacement value is displayed as a  $3 \times 12 = 36$  mm displacement, for example.

The Von Mises stress results are shown in form of color maps. The units are in megapascals. Additionally, one screenshot, fig. 5.2.3, shows the safety factor against yielding mapped on the side plates on the original frame. This color map has no units.

## 5.1 Displacements: original frame

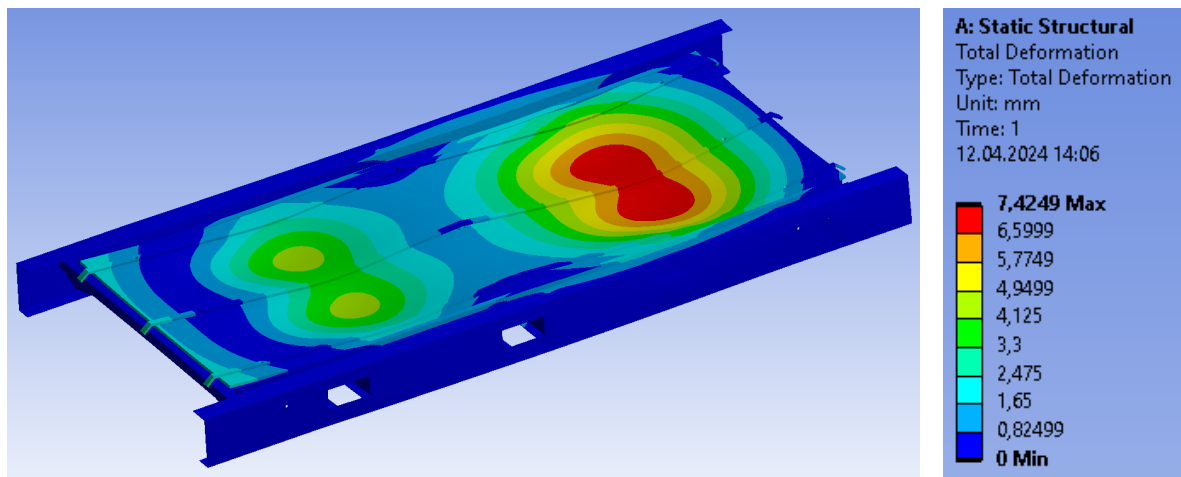


Figure 5.1.1 Total deformation overview. Screenshot from Ansys Mechanical [13].

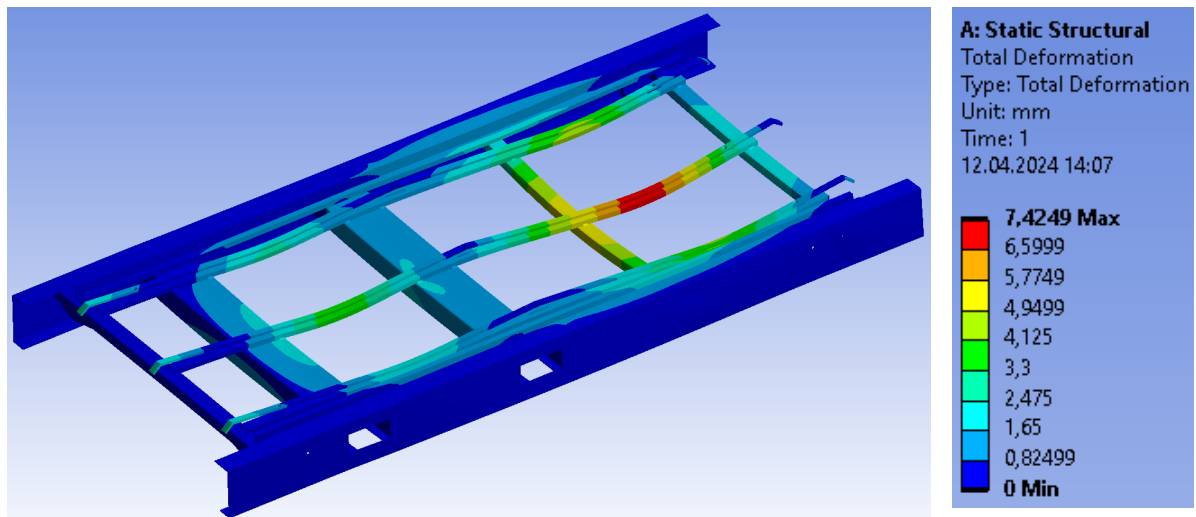


Figure 5.1.2 Total deformation overview. Plywood plate hidden. Screenshot from Ansys Mechanical [13].

One can see that the maximum displacements are located where the bale loads are applied. The maximum is ca. 7,4 mm, which is shown as the red area where the weight of the bale in the back acts. The side plates show generally small displacements, but towards the back there is an area with displacements in the region of 1,6 - 3,3 mm.

## 5.2 Von Mises stress: original frame

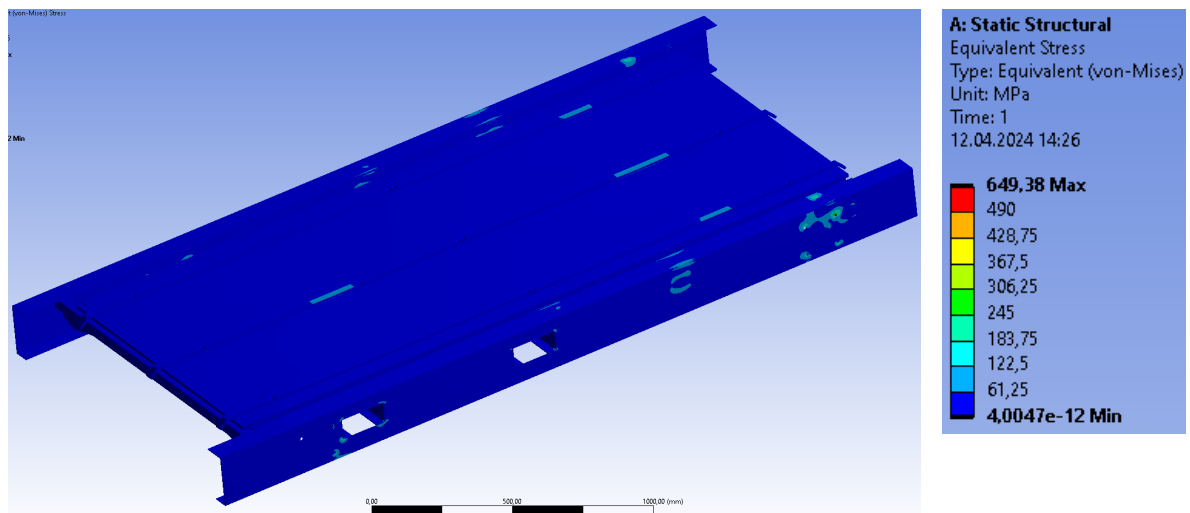


Figure 5.2.1 Von Mises stress overview. Screenshot from Ansys Mechanical [13].

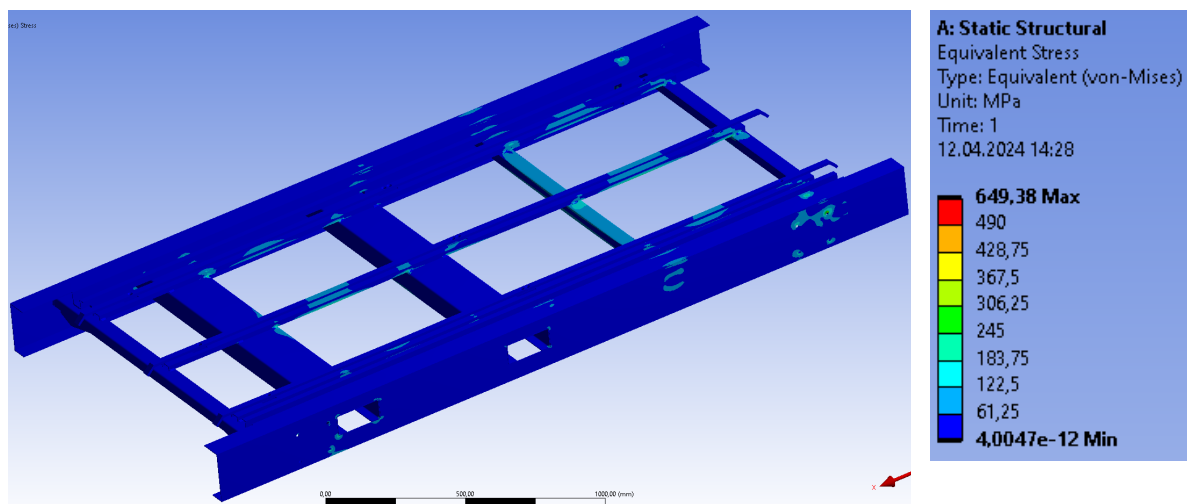


Figure 5.2.2 Von Mises stress overview. Plywood plate hidden. Screenshot from Ansys Mechanical [13].

One can see that the Von Mises stress is generally low, but at points of contacts and at bolt holes, there are stress concentrations with high values, for example in the region of 240-650 MPa.

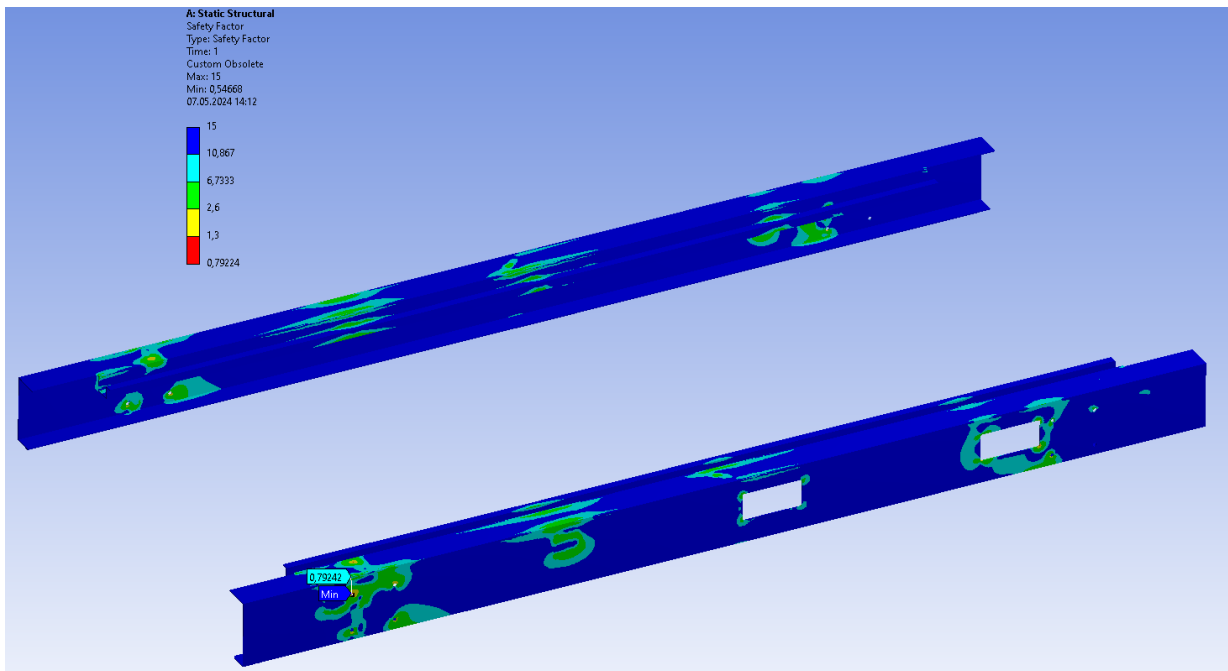


Figure 5.2.3 Safety factor mapped onto the side plates according to Von Mises yield criterion. Yield stress of 355 MPa is used as limit. Screenshot from Ansys Mechanical [13].

The above screenshot shows the safety factor against yielding for the side plates. One observes that the safety factor is generally in the region of 10-15, but at certain areas the factor drops towards 2,6. Only few critical areas show a safety factor below 2,6. This includes the bolt holes and where the plates are welded to other parts. Here follows screenshots of Von Mises stresses at critical locations.

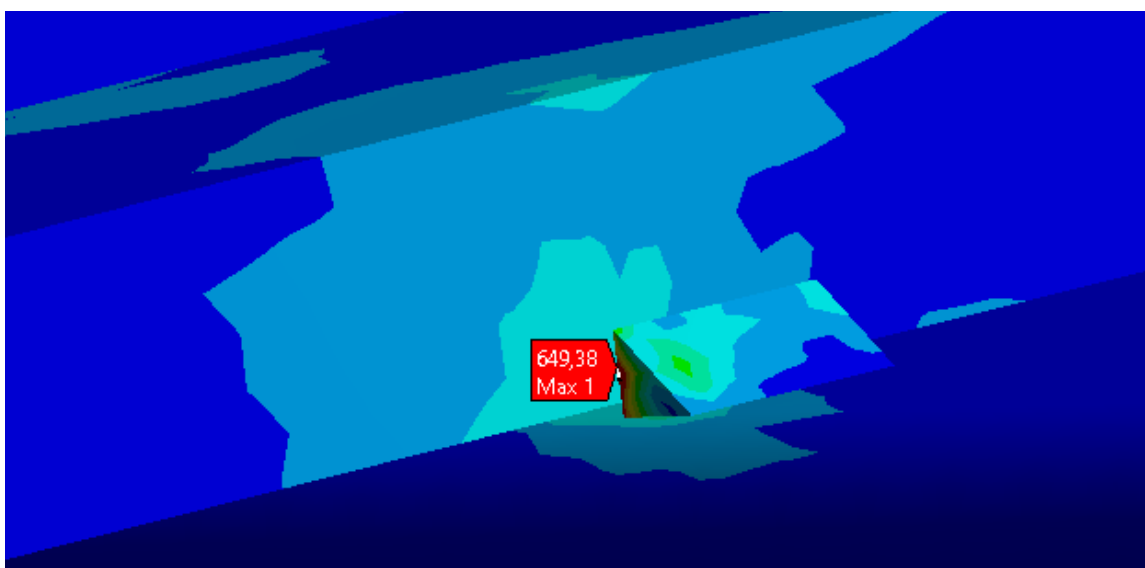


Figure 5.2.4 Von Mises stress max value of 649,38 MPa at welded connection. Screenshot from Ansys Mechanical [13].

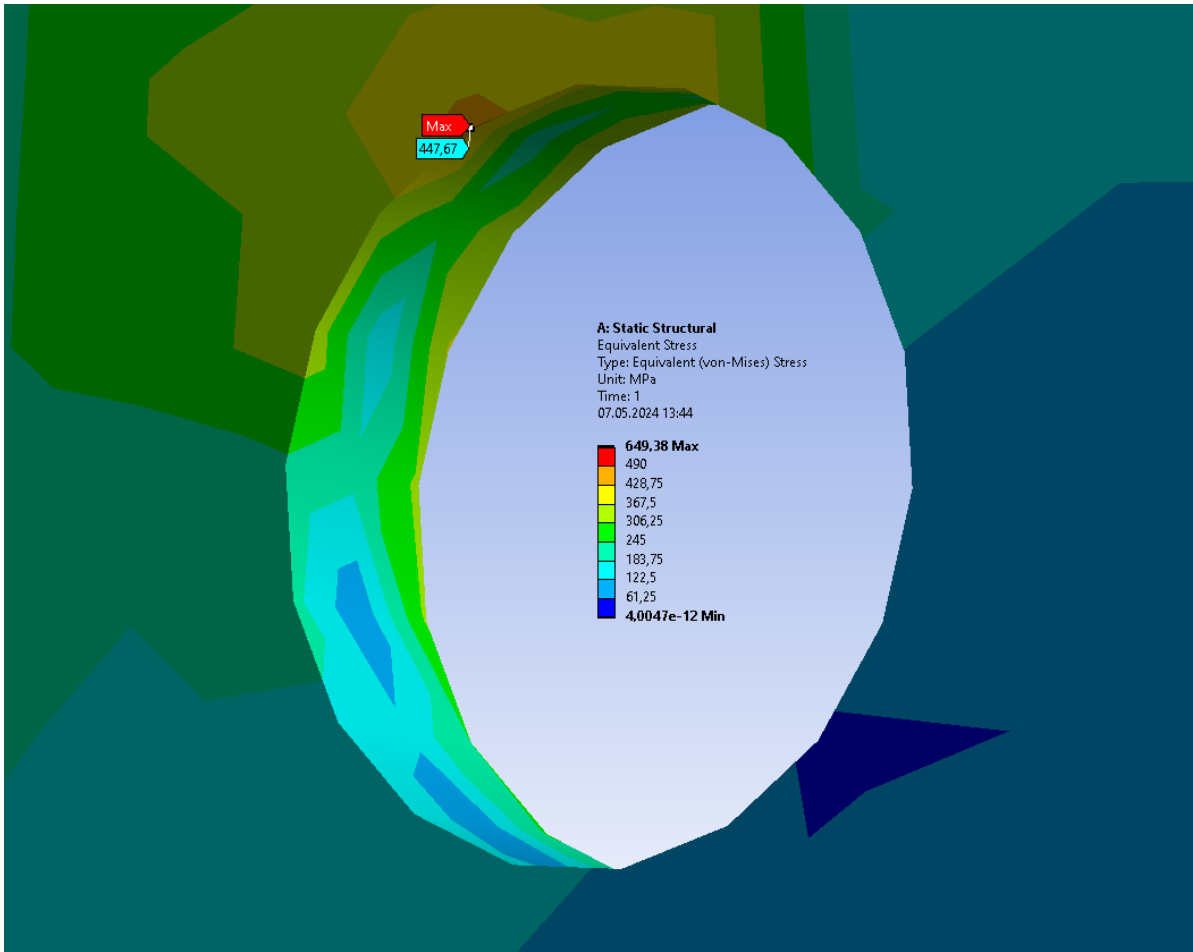


Figure 5.2.5 Von Mises stress value of 447,67 MPa at bolt hole. Screenshot from Ansys Mechanical [13].

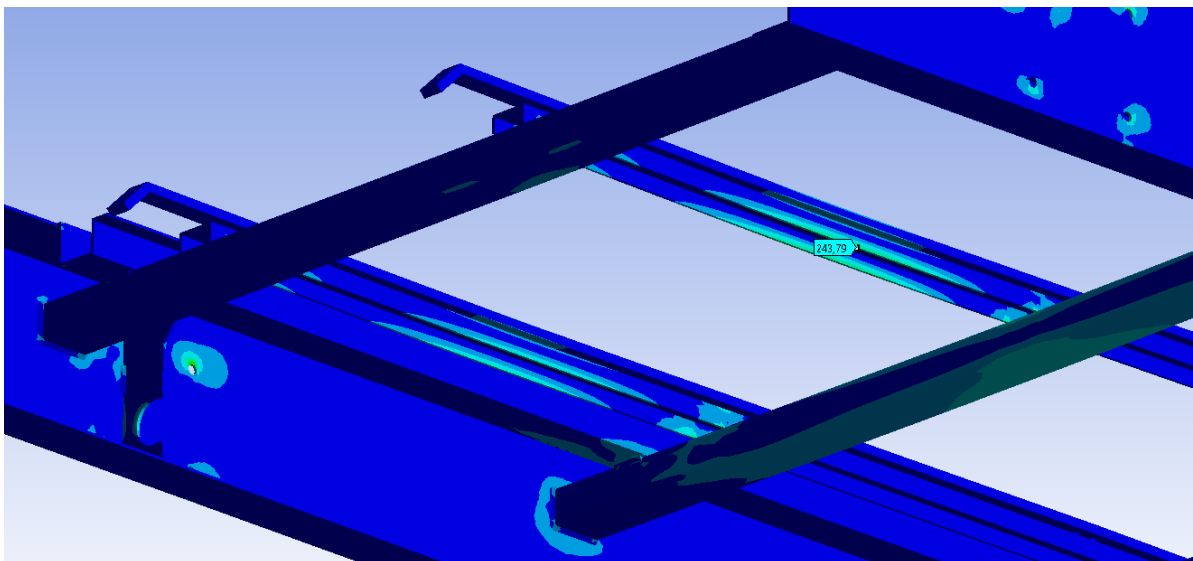
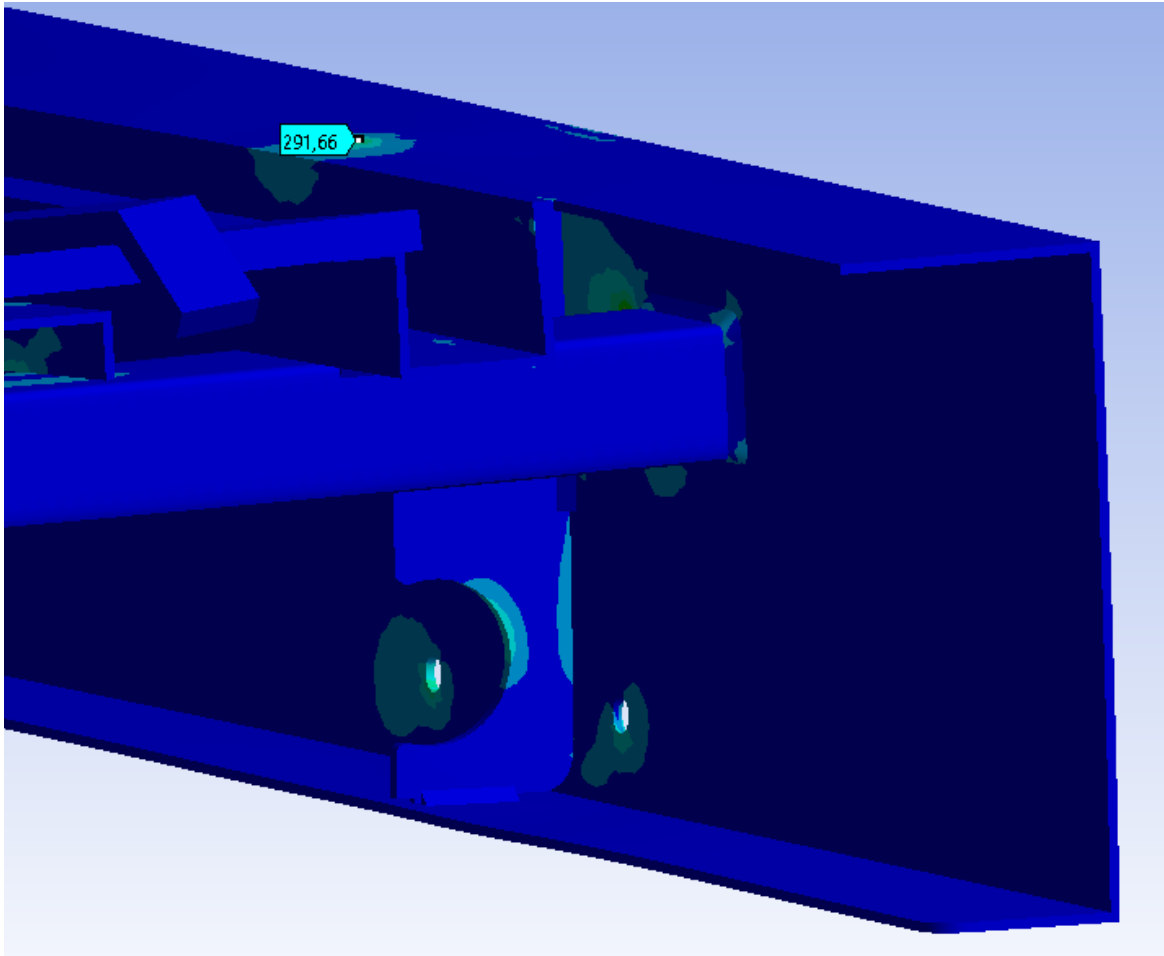


Figure 5.2.6 Von Mises stress value of 243,79 MPa at point of maximum displacement. Screenshot from Ansys Mechanical [13].



*Figure 5.2.7 Von Mises stress value of 291,66 MPa at connection between side plate and reinforcement plate. Screenshot from Ansys Mechanical [13].*

### 5.3 Displacements: optimized frame

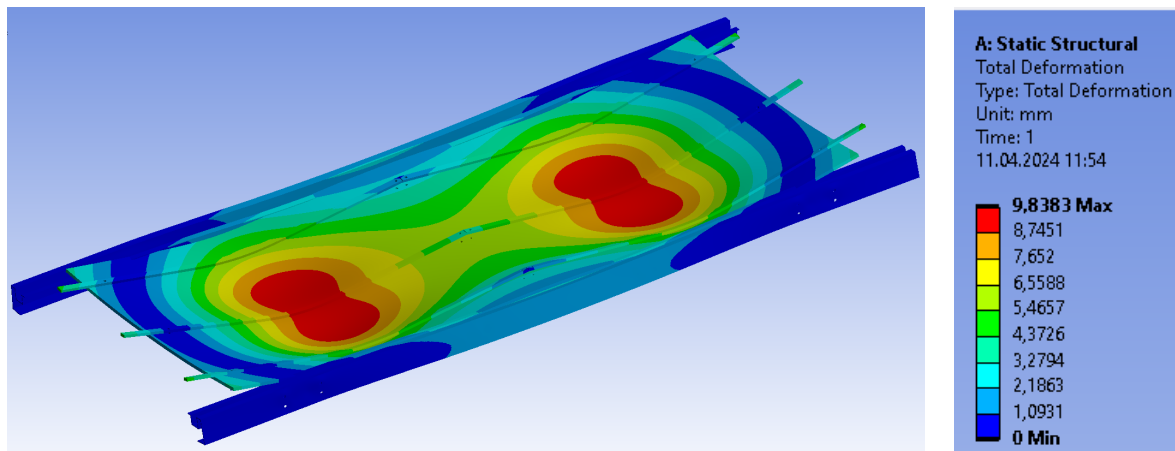


Figure 5.3.1 Total deformation overview. Screenshot from Ansys Mechanical [13].

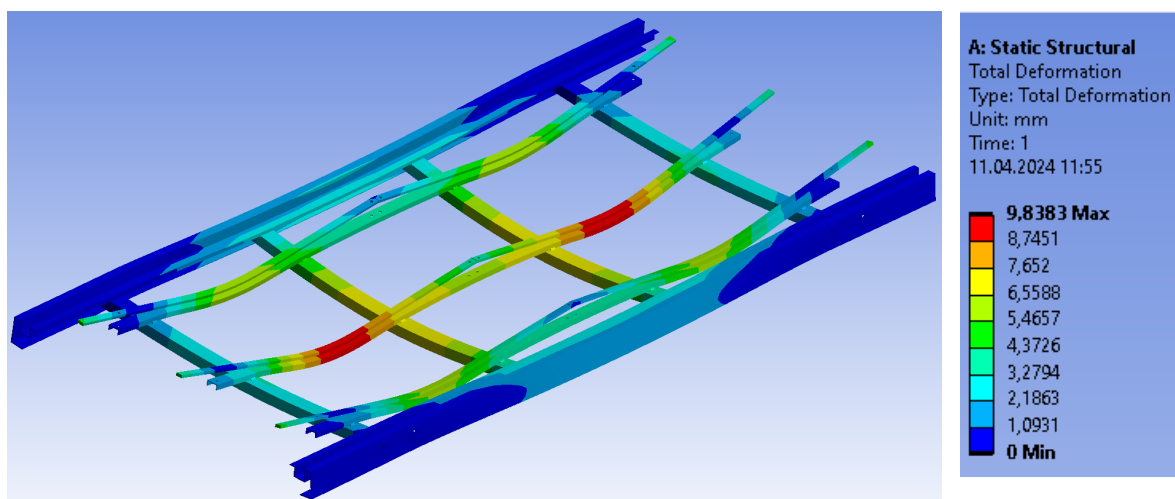


Figure 5.3.2 Total deformation overview. Plywood plate hidden. Screenshot from Ansys Mechanical [13].

On the optimized frame, one can see that here too, the maximum displacements are located where the bale loads are applied. The maximum is ca. 9,8 mm, which is located within the red areas. The side plates show some displacements at the middle, in the region between 2 and 4,5 mm approximately.

## 5.4 Von Mises stress: optimized frame

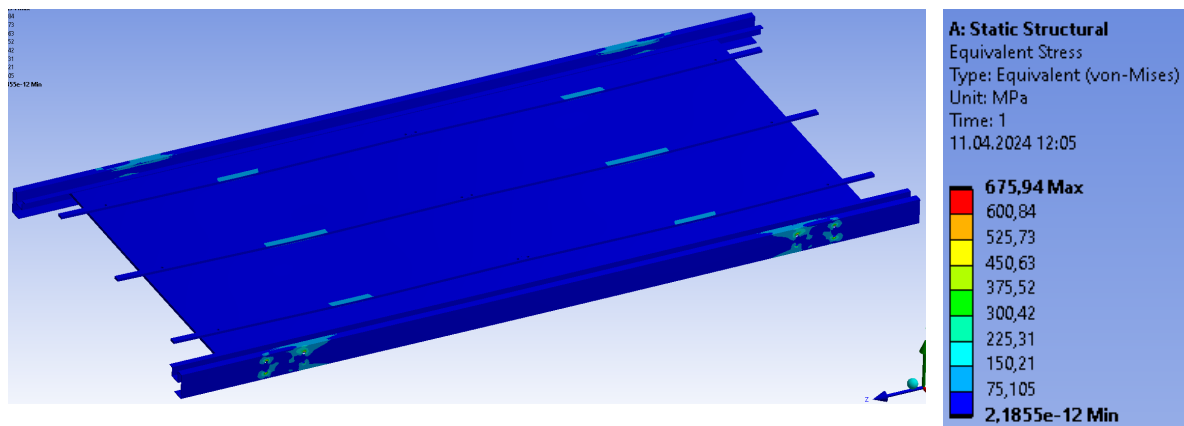


Figure 5.4.1 Von Mises stress overview. Screenshot from Ansys Mechanical [13].

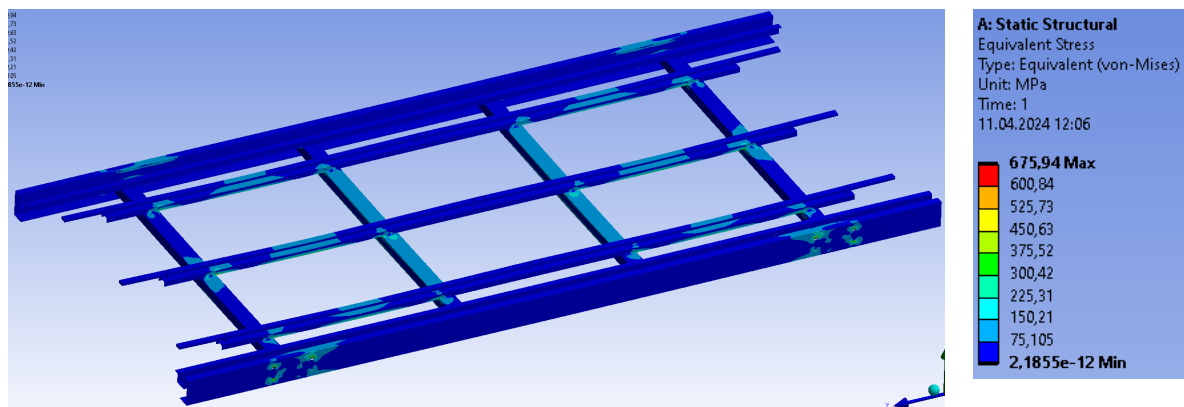


Figure 5.4.2 Von Mises stress overview. Plywood plate hidden. Screenshot from Ansys Mechanical [13].

The Von Mises stress is generally low, but certain regions exceed 150 MPa. At critical locations, like contacts and bolt holes, the stress is high, in the region above 375 MPa and reaching 675 MPa. Here follows screenshots of Von Mises stresses at critical locations.



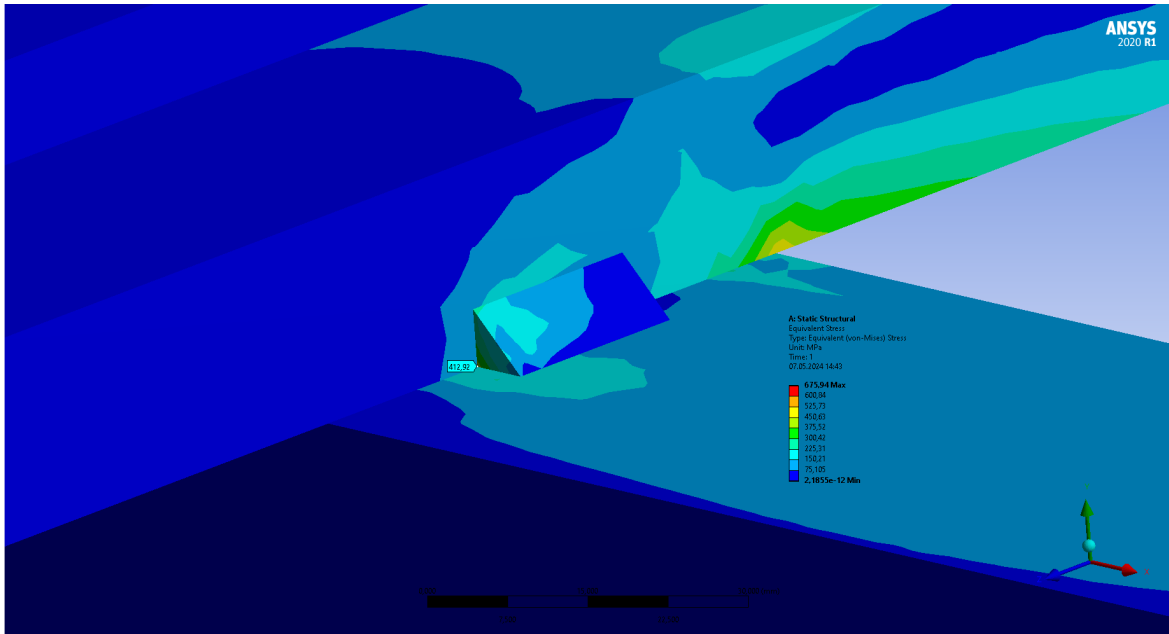


Figure 5.4.3 Von Mises stress value of 412,92 MPa at welded connection. Screenshot from Ansys Mechanical [13].

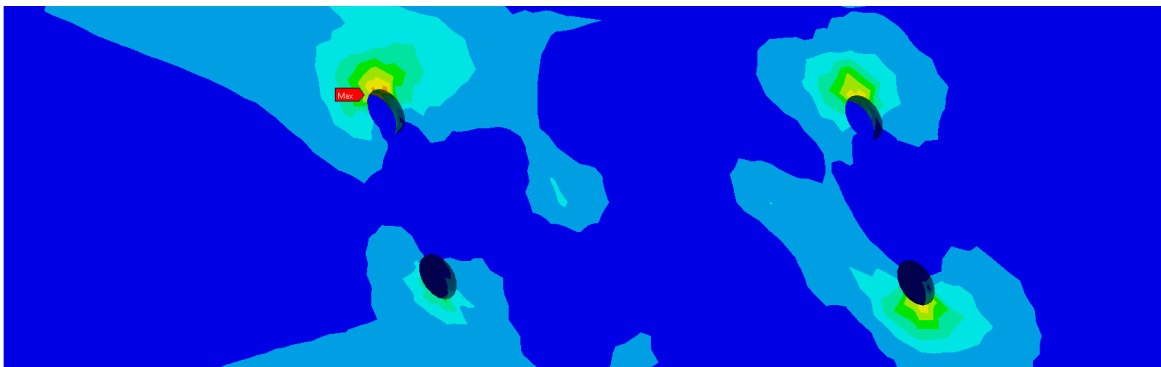


Figure 5.4.4 Von Mises maximum stress value of 675,94 MPa in bolt hole. Screenshot from Ansys Mechanical [13].

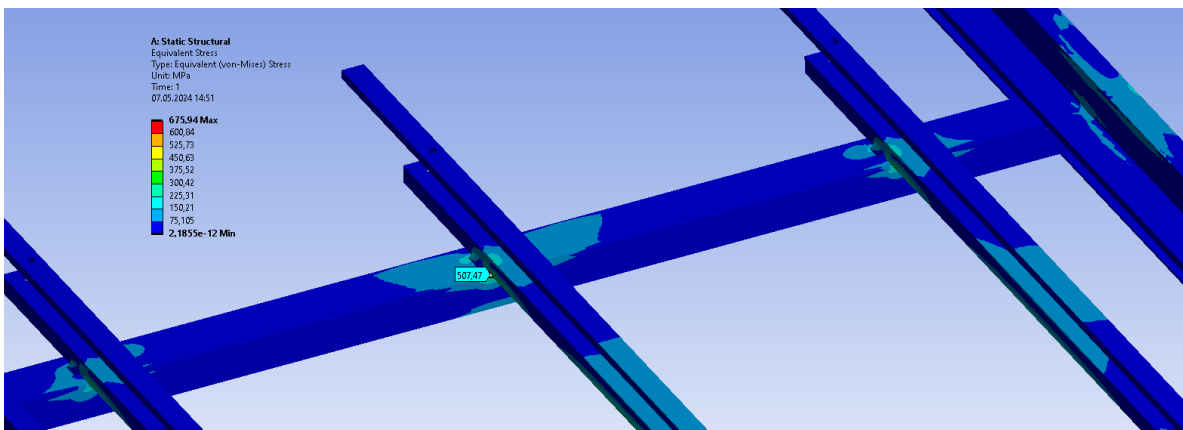


Figure 5.4.5 Von Mises stress value of 507,47 MPa at point of contact between two crossing profiles. Screenshot from Ansys Mechanical [13].

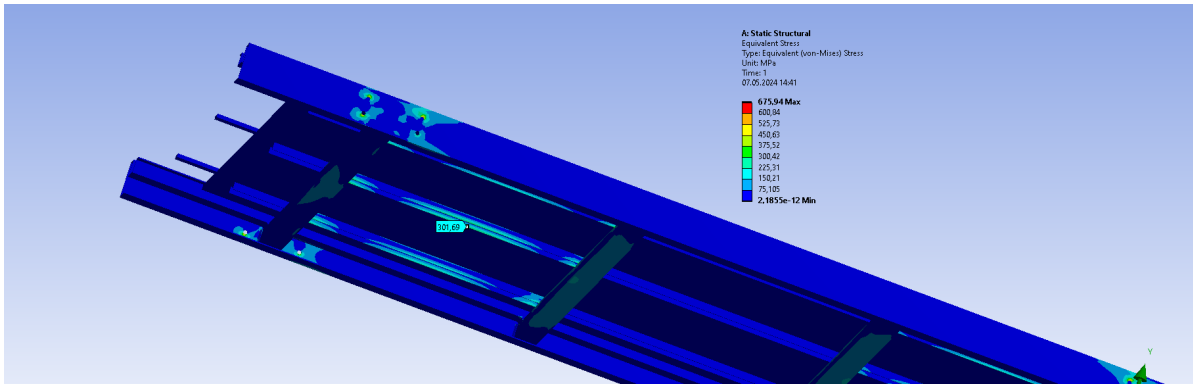


Figure 5.4.6 Von Mises stress value of 301,69 MPa at point of maximum displacement. Screenshot from Ansys Mechanical [13].

## 6 Discussion

### 6.1 Validity of results

The FEM results are approximate. The results depend on mesh quality, mesh density and which element type one uses. Additionally, Ansys Mechanical has very many options and for a beginner, there is much to learn.

A test is done which gives a picture of the uncertainty associated with the simulations. A beam with the same profile and mesh density as one used in the frames was modeled. It was meshed using default element types (SOLID186 and SURF154). The beam was analyzed for normal stresses due to bending, both in Ansys Mechanical and with analytic formulas. It was simply supported and a downwards acting force in the middle was applied. The results showed a deviation of ca. 13% when comparing the values of normal stress at the middle of the beam. Farther away from where the force was applied, at  $\frac{1}{4}$  of the beam length, the results compared to ca. 0,10%. This test indicates that the simulation setup produced satisfactory results, which gives credibility to the simulations on the frames. One can expect deviations at least within 13% between the FEM results and the real-life behavior of the frame structures. Calculations and FEM results for this test are documented in the appendix sections A5 and A6.

Another test to check the validity of the results is done. The support reactions of the original frame were extracted from the analysis, summed, and compared to the sum of the external forces applied. The frame is in static equilibrium, and therefore the value of these two summations should be equal in magnitude. The results show a maximum deviation of 0,7 Newtons, which is minimal compared to the forces applied. This test also gives satisfactory results and gives credibility to the frame simulations. The equilibrium check is given in the appendix section A7.

## 6.2 Reasonability of results

The results show the largest downwards displacements where the bale loads are applied. The maximum is ca. 7,4 mm on the original frame and 9,8 mm on the optimized. Here the beam/channel profiles supporting the load have quite small cross sections, and therefore, significant displacements values are reasonable.

For both frames, the Von Mises stress is generally lower than the yield stress by a margin. This makes sense, especially since the original frame is in use today. However, the results show high stress concentrations at the supports (bolt holes in outer side) and at other connections and contact points. This is the case for both frames and is also reasonable, but the stresses are quite high and above the yield limit.

Bolt connections fastening the plywood plate and glide rails to the frame were modeled with bonded contacts. However, the displacement results, at least on the optimized frame, seems to indicate that in the areas of the bolts, the parts have separated. That should not be the case, and consequently, the displacements in these areas are too high. This malfunction is not considered to be of significance for the interpretation of the other results.

## 6.3 Results in relevant regions assessed

### 6.3.1 Side plates on the original frame

The results show that the side plates on the original frame in general are safe with respect to yielding. The safety factor in most places is above 2,6, indicating that the plates could withstand more than a doubled load. This gives an indication that the side plates are oversized, and a size reduction is relevant. However, at contact areas and around bolt holes, the stresses exceed the yield stress.

### 6.3.2 Side plates on the optimized frame

The results show that the side plates on the optimized frame performs similar to those on the original frame when comparing Von Mises stresses. Again, the overall plates show no danger of yielding as the stresses are low compared to the yield stress. However, as on the original frame, stress concentrations exist at the bolt holes and at connection points to other parts. The bolt holes show even higher stresses than in the original frame. These stress concentrations in critical areas should not be overseen as failure may occur in such areas.

### 6.3.3 Area of maximum displacements

The displacement results show that both the original and the optimized frame experience the maximum downwards displacements where the bale loads are applied, 7,4 and 9,8 mm respectively. In these zones, on the bottom channel rail, the Von Mises stress is maximum 244 and 302 MPa respectively. Here, the safety factor against yielding is calculated to be 1,45 and 1,18 respectively. Even though the displacement values are significant in magnitude, the stresses here are within the 355 MPa limit, giving the impression that these zones are safe with respect to yielding if the loads never exceed the simulated loads. The profiles experiencing these large displacements and high stresses are small and thin. A general improvement proposal is to use larger dimensions, increased thickness and using a cross section with a height larger than the width (fig. 6.3.3.1), which is stronger against downward bending.

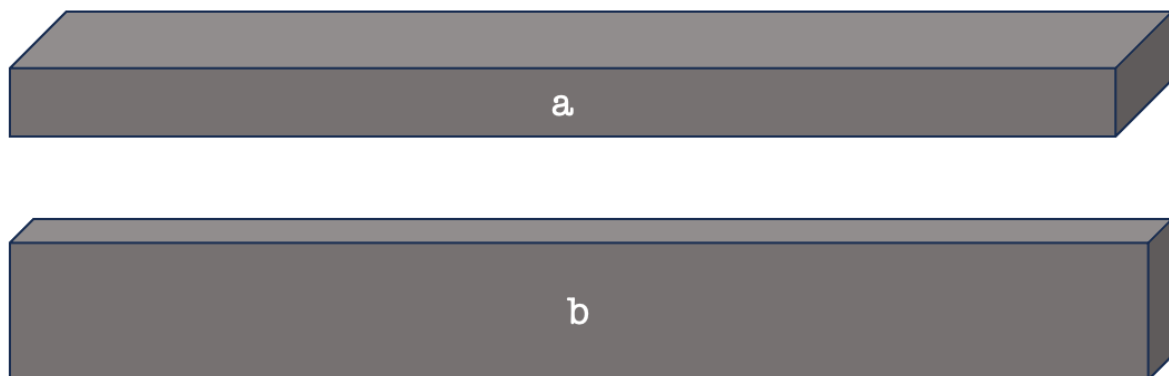


*Figure 6.3.3.1 Illustration: Profile “b” is more resistant to downwards bending than profile “a” due to a greater height-to-width ratio*

Additionally, beams could be mounted diagonally between the transverse beams to further reduce the displacements and stresses, fig. 6.3.3.2. However, this would increase material consumption significantly, which goes against the goal of cost-reduction.

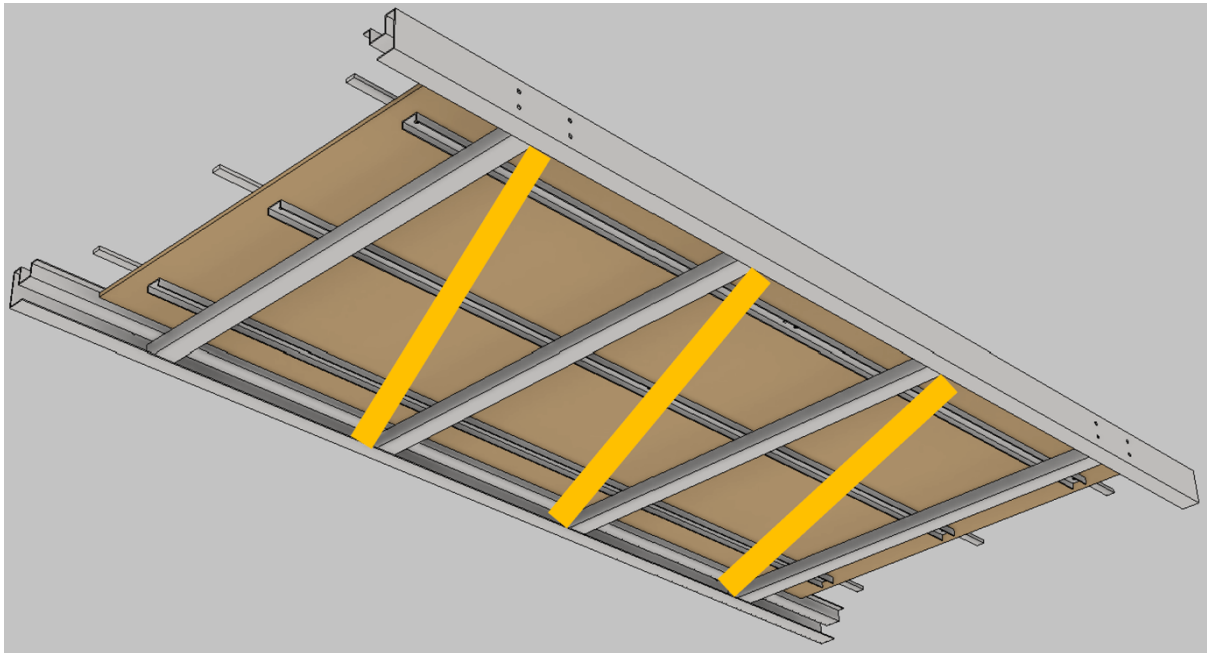


*Figure 6.3.3.2 Illustration: Orange beams mounted diagonally between transverse beams. Annotated screenshot from [15].*

### 6.3.4 Bolt holes in side plates

The results show high Von Mises stresses in the bolt holes for the floor stands. This is the case for both the original frame and the optimized. All weight is transferred to the bolts in these holes which cause large contact forces between the bolts and the holes. The maximum Von Mises stress values here, 448 MPa on the original frame and 676 MPa on the optimized frame, both exceed the yield stress, the latter almost by a factor of two. This is not acceptable. This region should be assessed closer.

Calculations using the theory presented in chapter 2.5 are performed to further validate the stresses acting between the bolt and the hole. The computations are given in the appendix. These calculations are minimally affected by uncertainty bound to the FEM simulations, like the mesh density and quality, and therefore gives a more exact result. To calculate the contact stress in the bolt/hole connection, one needs access to the contact force acting between the bolt and the hole. This force was extracted as a support reaction from the simulation on the optimized frame. The force was extracted from the bolt hole with the largest Von Mises stress result.

<input checked="" type="checkbox"/> Force Reaction 13 (Y) [N]	<input checked="" type="checkbox"/> Force Reaction 13 (Z) [N]
6209,6	15495

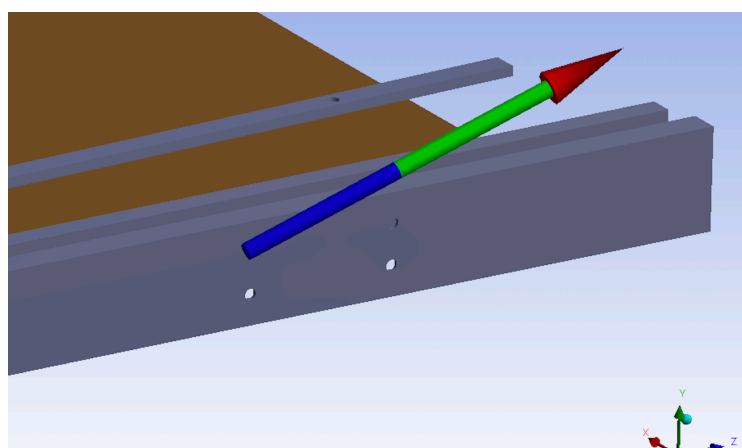


Figure 6.3.4.1 Resultant force in bolt hole with the highest stress. The magnitudes of the y- and z-component are shown in units of Newtons. Screenshot from Ansys Mechanical [13].



This resultant force is further used to compute the maximum shear stress in the contact between the bolt and hole. The maximum shear stress is calculated to be 395 MPa. The theory says that the maximum shear stress should not exceed the yield stress divided by two, for the contact area to be safe from yielding. In this case the limit is

$$\frac{\sigma_y}{2} = \frac{355}{2} = 177,5 \text{ MPa.}$$

This criteria is not met because

$$\tau_{max} = 395 > 177,5.$$

Both the FEM results and the analytic calculation therefore indicate that there is danger of yielding at the bolt connection for the floor stands.

Improvement proposals include adding extra plates to the side plates where the bolts are mounted. This would increase the thickness such that the hole depth becomes larger. In this way, the bolt and hole are in contact over a larger area, resulting in reduced stress. Such reinforcement plates could be welded to the side plates.

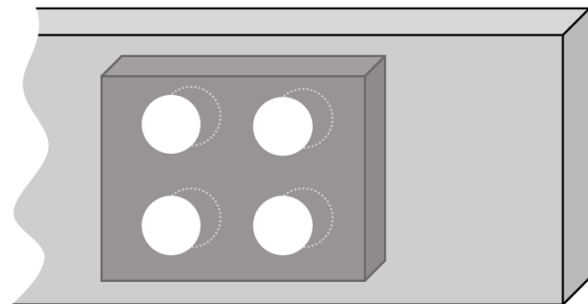


Figure 6.3.4.2 Illustration: dark grey reinforcement plate mounted to the side plates. Hole depth increased.

Additionally, larger bolts and holes would reduce stresses. Using the same contact stress calculation as above, the maximum shear stress at the contact reduces to 115 MPa when using a 6 mm thick extra plate and doubled bolt size. These measures contributed to reducing the maximum shear stress by a factor of 3,4 and a safety factor of 1,5 against yielding is achieved. Lastly, increasing the number of bolts and rounding the edges of the holes contribute to lower stresses.

### 6.3.5 Other contact points

The results show that high Von Mises stresses occur at certain contact points between parts. On the original frame a stress concentration of 292 MPa exist in the contact between the side plates and reinforcement plates. A stress concentration of 507 MPa exist around the contact between two crossing profiles in the optimized frame. These values are high, especially the latter which exceeds the yield stress by a factor of 1,4. One of the reasons that these high values occur may be due to the CAD models used in the FEM simulations having sharp edges. Rounding of edges can reduce the stresses some.

### 6.3.6 Weldments

The results show high stresses at certain weldments. Stresses of magnitude 649 MPa on the original frame and 413 MPa on the optimized frame occur at welds. Both values exceed the yield stress of 355 MPa, indicating that yielding is likely. However, the fillet welds used in the simulations are modeled as “hard” triangular prisms. On the real frame, the welds have a much more rounded profile. The simplified hard edges may be a big factor causing the stress concentrations to reach these high values. The simulations results are therefore limited to provide any detailed information on stresses at the weldments. However, a general proposal is to use large welds fastening the parts together.

## 7 Conclusion

The project is carried out successfully since the results give a basis for fulfilling the main goals of the project; 1) determine if the original frame is oversized and 2) determine if a smaller frame could perform equally well under the same load.

The results show that the side plates used in the original frame is oversized and there is potential for size reduction since the safety factor against yielding is mainly above 2,6 in these. The reduced side plates on the optimized frame also show general minimal Von Mises stresses which indicates that the size reduction was successful for carrying the same load. However, at critical areas such as weldments and contacts, local stress concentration exceeds the yield limit. Proposed measures to lower these stress concentrations in the side plates include:

- Rounded edges of bolt holes
- Extra plates where bolts are mounted to increase hole depth
- Larger bolts
- Larger welds

The results also showed that where the bale loads act, there is significant downwards displacement and Von Mises stress values. Proposed measures to improve include:

- Using profiles with a greater height-to-width ratio
- Mounting extra members diagonally between transverse beams

Additionally, high stress concentrations occur where parts are welded and where parts are in contact. That may be due to the simplified CAD models having sharp edges.

## 8. References

- [1] D. G. Pavlou, “Essentials of the Finite Element Method: For Mechanical and Structural Engineers”. Published in Oxford, UK: Elsevier/Academic Press, 2015
- [2] P. Tesdal, “report\_project” Unpublished project report, own work, MSK250: Elementmetoder, UiS, Stavanger, Norway, 2023/11.
- [3] Student lecture notes of lectures by D. G. Pavlou, MSK250: Elementmetoder, UiS, Stavanger, Norway, 2023, unpublished
- [4] R. C. Hibbeler, *Mechanics of Materials*, 10<sup>th</sup> edition in SI units. Harlow, UK: Pearson, 2018
- [5] Ansys Inc. “Equivalent stress”. Ansys.com. Retrieved from: [https://courses.ansys.com/wp-content/uploads/2019/04/1.3.4-Equivalent -Stress- -rebranded.pdf](https://courses.ansys.com/wp-content/uploads/2019/04/1.3.4-Equivalent-Stress-rebranded.pdf) Available 13.05.24 by search “von mises” in Ansys Innovation Space: <https://ansyskm.ansys.com/> (Latest accessed: 13.05.24)
- [6] A. P. Boresi, R. J. Schmidt, *Advanced Mechanics Of Materials*, 6<sup>th</sup> edition. Hoboken, US: Wiley, 2003
- [7] R. G. Budynas, J. K. Nisbett, *Shigley’s Mechanical Engineering Design*, 11<sup>th</sup> edition in SI units. McGraw Hill, 2021
- [8] Engineering Library. “Coefficient of Friction.” EngineeringLibrary.org. Retrieved from: <https://engineeringlibrary.org/reference/coefficient-of-friction> (Latest accessed: 12.05.24)

- [9] Engineers Edge. "Coefficient of Friction Equation and Table Chart." EngineersEdge.com. Retrieved from: [https://www.engineersedge.com/coefficients\\_of\\_friction.htm](https://www.engineersedge.com/coefficients_of_friction.htm) (Latest accessed: 12.05.24)
- [10] eMachineShop. "Coefficient of Friction." eMachineShop.com. Retrieved from: <https://www.emachineshop.com/coefficient-of-friction/> (Latest accessed: 12.05.24)
- [11] Mechead. "Ansys Contact Types and Explanations." Mechead.com. Retrieved from: <https://www.mechead.com/contact-types-and-behaviours-in-ansys/> (Latest accessed: 12.05.24)
- [12] *Ansys Workbench 2020 R1*, Ansys Inc. [software.] Accessed: spring 2024. Available: <https://www.ansys.com/products/ansys-workbench#tab1-1>
- [13] *Ansys Mechanical 2020 R1*, Ansys Inc. [software.] Accessed: spring 2024. Available: <https://www.ansys.com/products/structures/ansys-mechanical>
- [14] *Ansys Discovery SpaceClaim 2020 R1*, Ansys Inc. [software.] Accessed: spring 2024. Available: <https://www.ansys.com/products/3d-design/ansys-spaceclaim>
- [15] *Inventor Professional 2024*, Autodesk Inc. [software.] Accessed: spring 2024. Available: <https://www.autodesk.no/products/inventor/overview?term=1-YEAR&tab=subscription&plc=INVPROSA>
- [16] Matmatch. "EN 10149-2 Grade S355MC thermomechanically rolled." Matmatch.com. Retrieved from: <https://matmatch.com/materials/minfm32916-en-10149-2-grade-s355mc-thermomechanically-rolled>. (Latest accessed: 13.05.24)
- [17] Solid Mechanics Classroom. *Introduction to Finite Element Method (FEM) for Beginners*. (20.07.20). Latest accessed: 15.05.24. [Online Video.] Available: <https://www.youtube.com/watch?app=desktop&v=C6X9Ry02mPU>

# Acknowledgements

I want to express my thanks to the supervisors Atle Sjølyst-Kverneland (manager TKS AGRI AS) and Dimitrios Pavlou (professor UiS). They have both been positive and have helped me throughout the project. Thanks to Adugna Deressa Akessa (senior engineer UiS) for helping me to manage the complex FEA software and Jo Vegar Lunåsno (designer TKS AGRI AS) for providing technical information and CAD files.

# Appendix

## A.1 Geometry overview – original frame

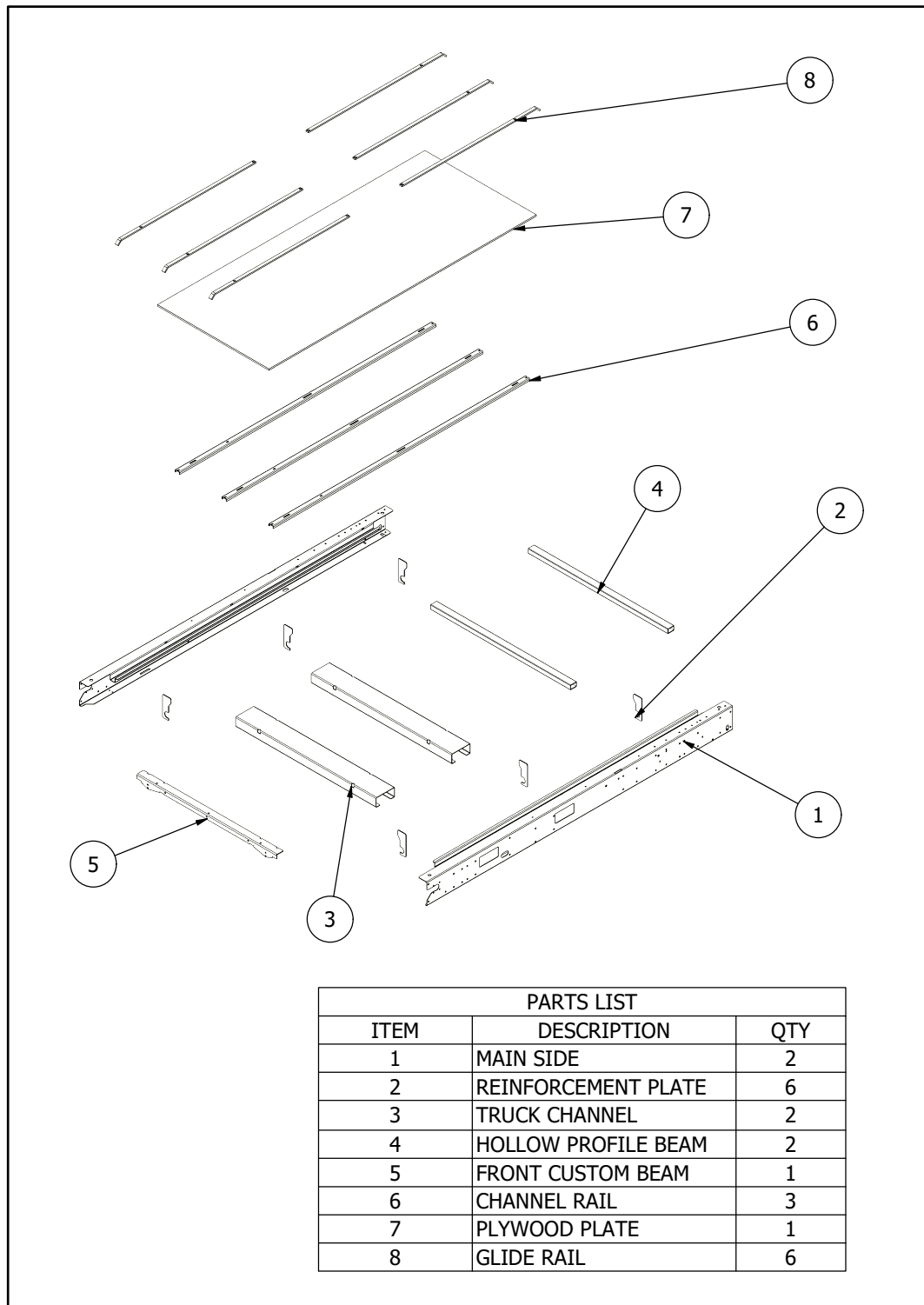


Figure A.1.1 Exploded view with parts list for simplified original frame. Produced in [15].

## A.2 Geometry overview – optimized frame

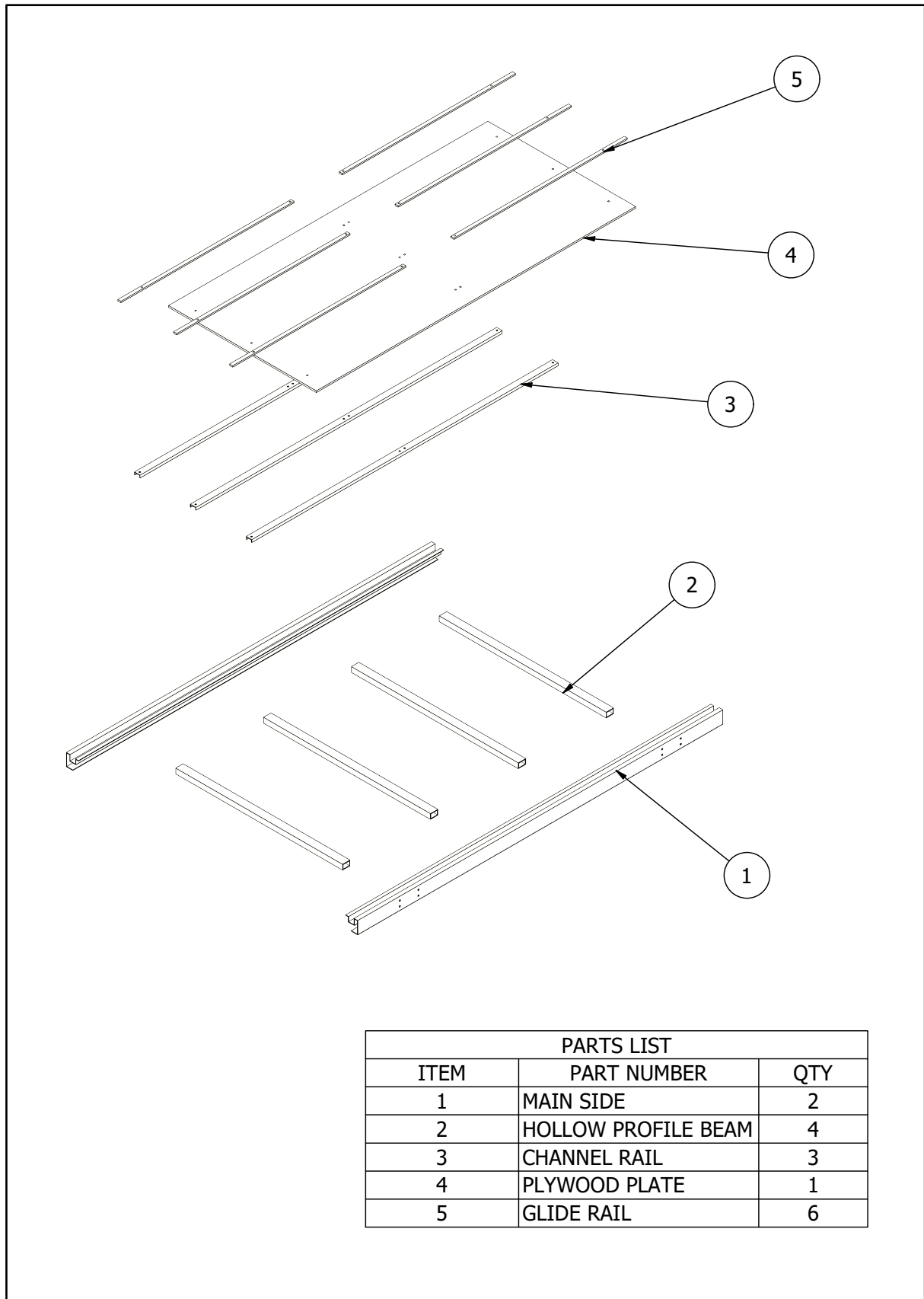


Figure A.2.1 Exploded view with parts list for optimized frame. Produced in [15].



## A.3 Bolt/hole contact stress calculation 1

**Forces:**

$$F_y = 6209,6 \text{ N}$$

$$F_z = 15495 \text{ N}$$

$F_x$  is not used since that is the force acting in the in/out-direction of the hole. It is only  $F_y$  and  $F_z$  that act as contact forces between the hole and the bolt.

**Resultant force:**

$$P = \sqrt{6209,6^2 + 15495^2} = 16692,94 \text{ N}$$

**Force per length where length is the thickness of the plate (3 mm):**

$$w = \frac{P}{h} = \frac{16692,94}{3 * 10^{-3}} = 5564313 \frac{\text{N}}{\text{m}}$$

$\Delta$ , where radius of hole is 5,5 mm and radius of bolt is 5,25 mm. Poisson's ratio is 0,29 and modulus of elasticity is 207,5 MPa for both the plate and bolt:

$$\begin{aligned} \Delta &= \frac{1}{\left(\frac{1}{2R_{hole}}\right) + \left(\frac{1}{2R_{bolt}}\right)} \left( \frac{1 - \nu_{plate}^2}{E_{plate}} + \frac{1 - \nu_{bolt}^2}{E_{bolt}} \right) \\ &= \frac{1}{\left(\frac{1}{2 * 5,5 * 10^{-3}}\right) + \left(\frac{1}{2 * 5,25 * 10^{-3}}\right)} * 2 * \frac{1 - 0,29^2}{207,5 * 10^9} \\ &= 2,039257 * 10^{-12} \frac{\text{m}}{\text{Pa}} \end{aligned}$$

**The contact width,  $b$ , using the previously calculated  $w$  and  $\Delta$ :**

$$b = \sqrt{\frac{2w\Delta}{\pi}} = \sqrt{\frac{2 * 5564313 * 2,039257 * 10^{-12}}{\pi}} = 0,002687706 \text{ m}$$

**The maximum shear stress using the previously calculated  $b$  and  $\Delta$ :**

$$\begin{aligned} \tau_{max} &= 0,300 \frac{b}{\Delta} = 0,300 * \frac{0,002687706}{2,039257 * 10^{-12}} = 395394900 \text{ Pa} \\ &\approx \underline{\underline{395 \text{ MPa}}} \end{aligned}$$

## A.4 Bolt/hole contact stress calculation 2 using triple plate thickness and doubled size bolts/holes

**Resultant force:**

Same as before.

$$P = 16692,94 \text{ N}$$

**Force per length where length is the thickness of the plate (9 mm):**

$$w = \frac{P}{h} = \frac{16692,94}{9 * 10^{-3}} = 1854771 \frac{\text{N}}{\text{m}}$$

$\Delta$ , where radius of hole is 10,75 mm and radius of bolt is 10,5 mm. Poisson's ratio is 0,29 and modulus of elasticity is 207,5 MPa for both the plate and bolt:

$$\begin{aligned} \Delta &= \frac{1}{\left(\frac{1}{2R_{hole}}\right) + \left(\frac{1}{2R_{bolt}}\right)} \left( \frac{1 - \nu_{plate}^2}{E_{plate}} + \frac{1 - \nu_{bolt}^2}{E_{bolt}} \right) \\ &= \frac{1}{\left(\frac{1}{2 * 10,75 * 10^{-3}}\right) + \left(\frac{1}{2 * 10,5 * 10^{-3}}\right)} * 2 * \frac{1 - 0,29^2}{207,5 * 10^9} \\ &= 7,971640 * 10^{-12} \frac{\text{m}}{\text{Pa}} \end{aligned}$$

**The contact width,  $b$ , using the previously calculated  $w$  and  $\Delta$ :**

$$b = \sqrt{\frac{2w\Delta}{\pi}} = \sqrt{\frac{2 * 1854771 * 7,971640 * 10^{-12}}{\pi}} = 0,003068026 \text{ m}$$

**The maximum shear stress using the previously calculated  $b$  and  $\Delta$ :**

$$\begin{aligned} \tau_{max} &= 0,300 \frac{b}{\Delta} = 0,300 * \frac{0,003068026}{7,971640 * 10^{-12}} = 115460300 \text{ Pa} \\ &\approx \underline{\underline{115 \text{ MPa}}} \end{aligned}$$

## A.5 Comparison FEM results with analytic calculations: Normal stress at the middle length of a simple beam

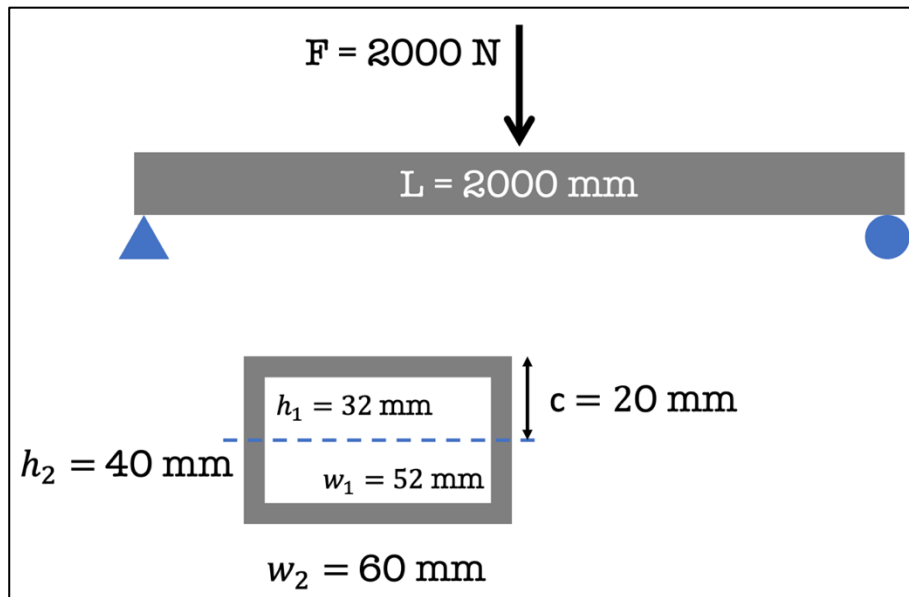


Figure A.5.1 Beam definitions. Simply supported. Concentrated load of 2000 N at the middle.

### Moment of inertia of cross section:

[4, appendix]

$$\begin{aligned}
 I_x &= \frac{w_2 h_2^3}{12} - \frac{w_1 h_1^3}{12} & (A.5.1) \\
 &= \frac{60 * 40^3}{12} - \frac{52 * 32^3}{12} \\
 &= 178005,3 \text{ mm}^4
 \end{aligned}$$

### Maximum bending moment (in the middle of the beam):

$$M = 1000 * \frac{L}{2} = 1000 * \frac{2000}{2} = 1 * 10^6 \text{ Nmm}$$

### Flexure formula for maximum normal stress at top/bottom of the beam at the middle length:

[4, p. 313]

$$\begin{aligned}
 \sigma_{max} &= \frac{Mc}{I_x} & (A.5.2) \\
 &= \frac{1 * 10^6 * 20}{178005,3} = 112,3562 \\
 &\approx \underline{\underline{112,36 \text{ MPa}}}
 \end{aligned}$$

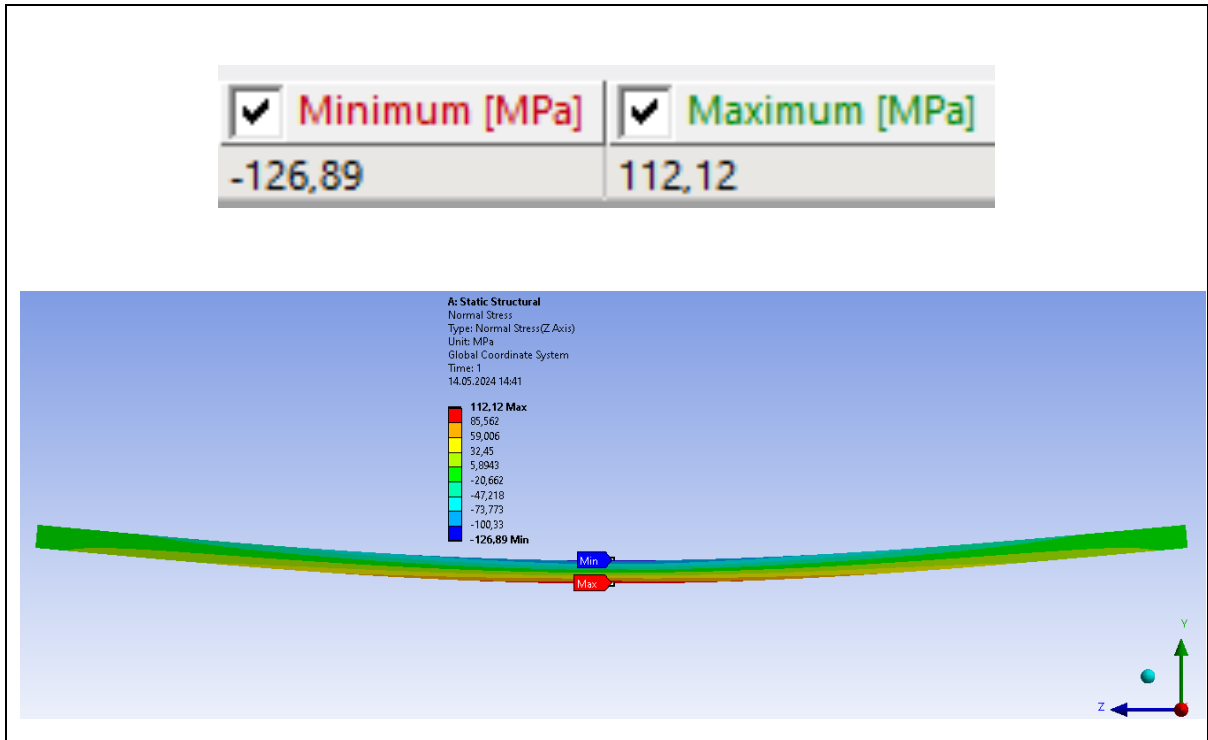


Figure A.5.2 FEM results: Normal stress of -126,89 MPa at the top and 112,12 MPa at the bottom at the middle length of the beam. Screenshot from Ansys Mechanical [13].

## A.6 Comparison FEM results with analytic calculations: Normal stress at the $\frac{1}{4}$ length of a simple beam

Bending moment in the  $\frac{1}{4}$  length of the beam:

$$M = 1000 * \frac{L}{4} = 1000 * \frac{2000}{4} = 5 * 10^5 \text{ Nmm}$$

Flexure formula for maximum normal stress at top/bottom of the beam at  $\frac{1}{4}$  length:

$$\begin{aligned}\sigma_{max} &= \frac{Mc}{I_x} \\ &= \frac{5 * 10^5 * 20}{178005,3} = 56,17810 \\ &\approx \underline{\underline{56,178 \text{ MPa}}}\end{aligned}$$

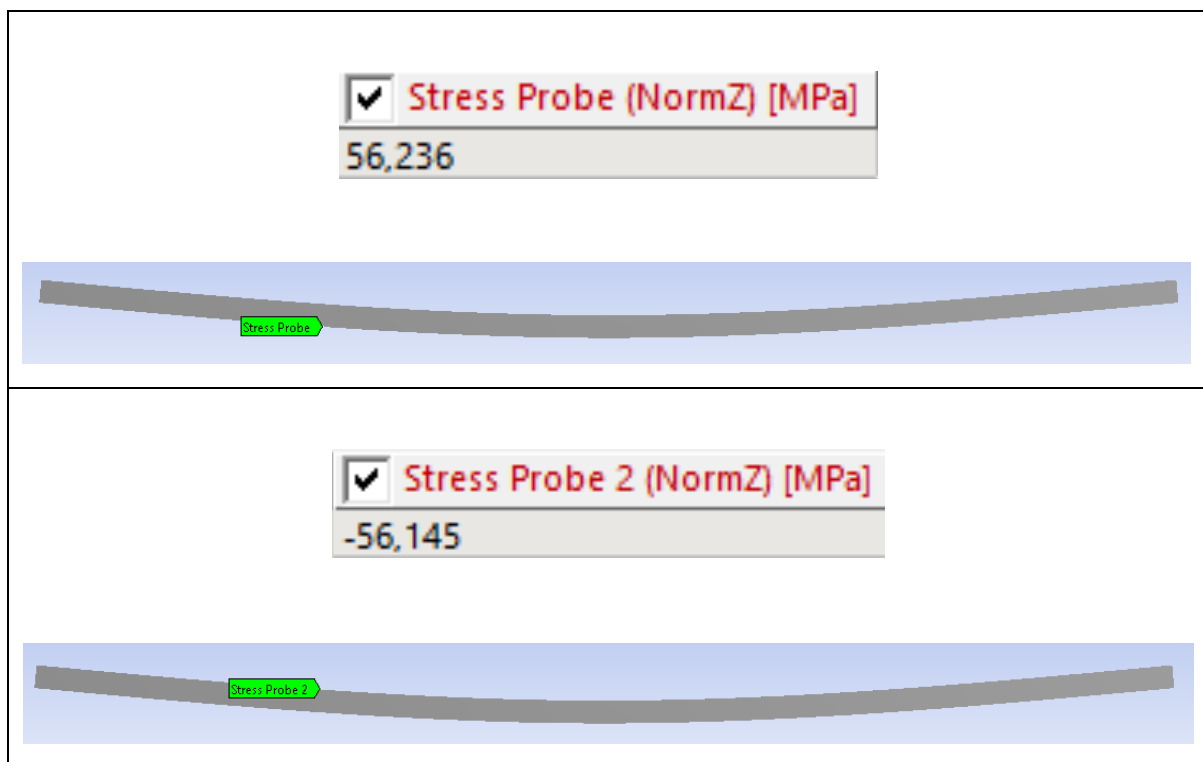


Figure A.6.1 FEM results: Normal stress of 56,236 MPa at the bottom and -56,145 MPa at the top at the  $\frac{1}{4}$  length of the beam. Screenshot from Ansys Mechanical [13].

## A.7 Equilibrium check for original frame

Table A.7.1 Sum of external forces compared to sum of support reactions. The last row is the deviations in Newtons.

<b>External forces</b>	<b>x</b>	<b>y</b>	<b>z</b>	
Bale 1 weight	0	0	-12000	
Bale 2 weight	0	0	-12000	
Machine weight	0	0	-7000	
Sum of external forces	0	0	-31000 N	
<b>Support reactions in bolt holes</b>	<b>x</b>	<b>y</b>	<b>z</b>	
Bolt hole 1	4669,1	153,26	-1925,8	
Bolt hole 2	3716,1	-13,462	6666,9	
Bolt hole 3	-1611,8	27,293	-1408,3	
Bolt hole 4	-6689,1	-209,65	4141,2	
Bolt hole 5	-8812,7	693,38	5529	
Bolt hole 6	-5469,1	2662,8	-1250,8	
Bolt hole 7	10857	-393,74	4705,3	
Bolt hole 8	3341,4	-1257,8	-957,42	
Bolt hole 9	-5477,8	-2663,8	-1231	
Bolt hole 10	-8811,7	-690,71	5536,1	
Bolt hole 11	3343,9	1257,6	-979,97	
Bolt hole 12	10862	391,72	4701,3	
Bolt hole 13	3715,9	12,315	6662,1	
Bolt hole 14	4666,3	-151,99	-1924	
Bolt hole 15	-6688,6	210,7	4143,1	
Bolt hole 16	-1611,6	-27,934	-1407,8	
Sum of support reactions	-0,7	-0,018	30999,91 N	
Deviations	-0,7	-0,018	-0,09 N	